Global Change Biology (2000), **6** (Suppl. 1), 84–115

Land–atmosphere energy exchange in Arctic tundra and boreal forest: available data and feedbacks to climate

WERNER EUGSTER,* WAYNE R. ROUSE,† ROGER A. PIELKE SR,‡ JOSEPH P. MCFADDEN,§ DENNIS D. BALDOCCHI,¶ TIMOTHY G. F. KITTEL,** F. STUART CHAPIN III§,**, GLEN E. LISTON,‡ PIER LUIGI VIDALE‡, EUGENE VAGANOV‡‡ and SCOTT CHAMBERS††

**Institute of Geography, University of Bern, Hallerstrasse 12, CH-3012 Bern, Switzerland, †School of Geography and Geology, McMaster University, Hamilton, ON L8S 4K1, Canada, ‡Department of Atmospheric Science, Colorado State University, Fort Collins, CO 80523-1371, USA, §Department of Integrative Biology, University of California, Berkeley, CA 94720-3140, USA, ¶NOAA/ERL/ATDD, PO Box 2456, Oak Ridge, TN 37831, USA, **National Center for Atmospheric Research, Boulder, CO 80307-3000, USA, ††Institute of Arctic Biology, University of Alaska, Fairbanks, AK 99775-7000, USA, ‡‡Institute of Forestry, Russian Academy of Sciences, Krasnoyarsk 660036, Russia*

Abstract

This paper summarizes and analyses available data on the surface energy balance of Arctic tundra and boreal forest. The complex interactions between ecosystems and their surface energy balance are also examined, including climatically induced shifts in ecosystem type that might amplify or reduce the effects of potential climatic change.

High latitudes are characterized by large annual changes in solar input. Albedo decreases strongly from winter, when the surface is snow-covered, to summer, especially in nonforested regions such as Arctic tundra and boreal wetlands. Evapotranspiration (Q_E) of high-latitude ecosystems is less than from a freely evaporating surface and decreases late in the season, when soil moisture declines, indicating stomatal control over Q_E, particularly in evergreen forests. Evergreen conifer forests have a canopy conductance half that of deciduous forests and consequently lower Q_E and higher sensible heat flux (Q_H). There is a broad overlap in energy partitioning between Arctic and boreal ecosystems, although Arctic ecosystems and light taiga generally have higher ground heat flux because there is less leaf and stem area to shade the ground surface, and the thermal gradient from the surface to permafrost is steeper.

Permafrost creates a strong heat sink in summer that reduces surface temperature and therefore heat flux to the atmosphere. Loss of permafrost would therefore amplify climatic warming. If warming caused an increase in productivity and leaf area, or fire caused a shift from evergreen to deciduous forest, this would increase Q_E and reduce Q_H. Potential future shifts in vegetation would have varying climate feedbacks, with largest effects caused by shifts from boreal conifer to shrubland or deciduous forest (or vice versa) and from Arctic coastal to wet tundra. An increase of logging activity in the boreal forests appears to reduce Q_E by roughly 50% with little change in Q_H, while the ground heat flux is strongly enhanced.

Keywords: Arctic tundra, boreal forest, circumpolar high-latitudes, climate feedbacks, eddy covariance flux data, surface energy balance

Correspondence: Werner Eugster, fax: +41 31 631-8511, e-mail: eugster@giub.unibe.ch

1 Introduction

The energy exchange between land, sea ice, and the atmosphere drives the Earth's climate system on local, regional, and ultimately, global scales. In order to assess the susceptibility and vulnerability of ecosystems to climate change, it is essential to understand the energy exchange processes at the Earth's surface and how they feed back to climate.

More than 15 years ago Ohmura (1982a,b,c,d) reviewed studies on the energy balance of Arctic tundra and concluded that the radiative exchange of the tundra region was relatively well understood, but its climate was not. Furthermore, Ohmura (1982a) suggested that the development of accurate boundary-layer models, which could be driven by synoptic or climatological data, would be an important step toward a better understanding of the tundra regional climate. Today such regional scale models exist (Pielke *et al*. 1992; Walsh *et al*. 1993; Lynch *et al*. 1995; Dethloff *et al*. 1996). However, these regional models require scenario input for modelling the changing climate of a region. This information can be supplied either as output from Global Climate Models (GCMs), or produced independently based on a range of changes in driving variables, which can be used as boundary conditions in regional models (e.g. Gyalistras & Fischlin 1999). In addition, scenarios of future regional climate changes in land surface properties caused by climate-driven vegetation change (Kittel *et al*. 2000) can be used to assess the susceptibility and vulnerability of ecosystems to such changes (e.g. Raupach *et al*. 1999).

The availability and reliability of the GCMs with which regional models can be integrated has improved in recent times. In general, the accuracy with which modern GCMs are able to represent current Arctic surface air temperatures, although regionally variable, is encouraging. For example, a comparison by Tao *et al*. (1996) of 10 years of data (1979–88) simulated by 19 GCMs, found that Arctic surface air temperatures can be predicted for North America with an accuracy of 2 °C regardless of season. Nonetheless, some crucial refinements to GCM parameterization schemes remain to be identified and implemented: (i) GCMs exhibit considerable underestimation of solar input at high latitudes (Wild *et al*. 1995) compared to observations by the global energy balance archive stations (Ohmura *et al*. 1989, 1993b; Ohmura & Gilgen 1993a). This underestimation is a result of the inadequate parameterization of cloud radiative properties (Wild *et al*. 1995; Rinke *et al*. 1997). The errors in the simulated fluxes under present climate are currently of a similar or larger magnitude than the simulated changes of these quantities with simulations of climate change (Wild *et al*. 1997). (ii) The cold bias of Arctic surface air temperatures in spring is a problem common to all GCMs, and is strongest in the models that do not account for vegetative masking of the high-albedo snow (Tao *et al*. 1996). Consequently, the credibility of GCM scenarios is lowest for the season which is most critical for the development of the plants at high latitudes, and where effects of a warming climate have already been identified (Keeling *et al*. 1996; Keyser *et al*. 2000). (iii) Land-surface parameterization schemes typically used in GCMs are sensitive in a nonlinear way to parameters which are aggregated from high-resolution data to the coarser resolution of the GCM. For example, GCMs are sensitive to an initial increase in forest cover in a transition from a simulation of homogeneous tundra to one of homogeneous coniferous forest (Pitman 1995). This problem can be minimized by incorporating secondary vegetation types in GCM grid cells instead of using only the model parameters of the dominant vegetation (Pitman 1995).

The aims of this paper are therefore: (i) to identify the necessary information to help assess the susceptibility and vulnerability of high-latitude ecosystems to climate change; (ii) to summarize available field data from surface energy balance studies that describe northern ecosystems; (iii) to characterize the surface energy balance of the circumpolar Arctic and boreal biomes; and (iv) to examine how possible changes in climate and ecosystem distribution may feed back to climate, based on a susceptibility–vulnerability approach. Section 2 describes the unique physical attributes of high-latitude ecosystems, and the consequences thereof. Section 3 summarizes available knowledge about the components involved in the surface energy balance of the boreal and Arctic climate zone. Section 4 presents a compilation of available data for summer conditions. In Section 5 potential feedbacks to local and regional climate are discussed, and an attempt is made to identify the shifts in vegetation type that would most strongly feed back to climatic change via the associated changes in surface energy partitioning.

2 Climatic conditions in the boreal and Arctic zones

The following analysis focuses on the large circumpolar terrestrial zone in the northern hemisphere at latitudes greater than ≈50°N, which consists of three regions: (i) the *boreal zone*, which ranges from close-crowned to open-canopy forest; (ii) the *subarctic zone* near the Arctic treeline, in which the forest is very open and trees are stunted or absent; and (iii) the *Arctic zone*, which consist of treeless tundra. Within this geographically diverse region there is a broad range of climate and physical characteristics of the land surface.

Table 1 Average climate data for North American stations in the Boreal zone (compiled from Hare & Hay 1974; Hare & Thomas 1979). K↓: solar radiation (W m^{-2}), average of the years 1962–76 (Canadian stations) or 1956–64 (US stations); T_m: mean temperature (°C); P: precipitation 1942–72 (mm); Sn: snowfall 1941–62 (cm); Cl: cloudiness 1942–72 (tenths); Dir: most frequent wind direction 1942–72; u: mean wind speed 1942–72 (m s^{-1})

	J	F	M	A	M	J	J	A	S	O	N	D	year
Boreal Zone													
Anchorage (61°10′ N, 199°59′ W)													
K↓	16	56	130	189	213	224	201	154	98	54	21	8	114
T_m	–10.9	–7.8	–4.8	2.1	7.7	12.5	13.9	13.1	8.8	1.7	–5.4	–9.8	1.8
P	20	18	13	11	13	25	47	65	64	47	26	24	374
Sn	27	25	21	8	1	0	0	0	0	14	25	31	156
Cl	6.7	6.8	6.7	6.9	7.6	7.6	7.5	7.8	7.8	7.8	7.2	7.3	7.3
Dir	NE	N	N	N	S	S	S	NW	NE	N	N	NE	N
u	2.3	2.6	2.6	2.5	2.9	2.8	2.5	2.3	2.3	2.4	2.3	2.2	2.5
Edmonton (53°34′ N, 113°31′ W)													
K↓	42	81	146	203	240	253	261	209	147	92	47	31	146
T_m	–14.1	–11.6	–5.5	4.2	11.2	14.3	17.3	15.6	10.8	5.1	–4.2	–10.4	2.7
P	24	20	21	28	46	80	85	65	34	23	22	25	473
Sn	24	19	20	15	3	0	0	0	2	10	19	24	137
Cl	6.5	6.5	6.4	6.4	6.4	6.7	5.8	5.7	5.8	5.9	6.3	6.4	6.2
Dir	S	S	S	S	S	NW	NW	S	S	S	S	S	S
u	3.5	3.6	4.0	4.8	4.7	4.4	4.0	3.7	4.0	4.0	3.6	3.3	4.0
Goose Bay (53°19′ N, 60°25′ W)													
K↓	39	81	136	190	209	221	212	174	126	76	38	30	128
T_m	–16.6	–14.9	–8.4	–1.6	5.1	11.9	16.3	14.7	10.1	3.2	–4.4	–12.9	0.2
P	72	63	68	62	56	72	84	91	76	63	67	63	837
Sn	70	61	64	48	18	2	0	0	3	25	51	59	400
Cl	6.3	6.3	6.3	7.3	7.5	7.6	7.5	7.1	7.1	7.4	7.3	6.4	7.0
Dir	W	W	W	NE	NE	NE	SW	W	W	W	W	W	W
u	4.8	4.4	4.5	4.4	4.2	3.9	3.8	3.8	4.2	4.5	4.2	4.4	4.3

2.1 Regional climate

In North America, excluding the ice cap areas in the eastern Queen Elizabeth Islands (Canada), annual mean temperature spans 21 °C (–18 to +3 °C), annual precipitation (in the few places it is measured) ranges from 60 to 460 mm, the frost-free period from 10 to 125 days, the median snow-free period from 80 to 245 days, and the annual average global radiation from 90 to 160 W m^{-2} (Hare & Thomas 1979). Annual average net radiation at the surface varies from 3 to 53 W m^{-2} (Rouse 1993).

A range of climatic parameters for typical North American stations, ranging from west to east in each of the three geographical zones, is given in Tables 1–3. Eurasia is much more continental with colder winters and warmer summers in central Siberia. There is a strong gradient from West to East in continentality, especially in rainfall, while the Hudson Bay moderates the climate at comparable latitudes in North America (Rouse 2000). Progressing northward from the boreal to the Arctic zone, there is a steady decrease in solar insolation, a marked decrease in mean annual temperatures, an increase in the number of winter months, a marked decline in precipitation, with a higher proportion occurring in the three summer months, and an increase in wind speeds (Tables 1–3). For all regions the average annual cloud cover is greater than 6/10 and exceeds 7/10 in the three summer months.

For most of the study area, snow comprises 40–80% of the annual precipitation, the majority of which is stored on the ground for six to nine months of the year. Actual snowfall may be two to three times that measured by standard snow collectors at weather stations, due to undercatch during windy periods, as well as to large numbers of trace events (Goodison 1981; Woo *et al*. 1983). Both of these factors are enhanced in the windswept tundra.

2.2 Physical characteristics of northern ecosystems

The magnitude and pattern of snow accumulation in high latitudes is poorly understood, but is strongly influenced by canopy and topographic heterogeneity at a variety of scales (Section 5.3). Intercepted snow within

Table 2 As Table 1 but for the Subarctic zone

	J	F	M	A	M	J	J	A	S	O	N	D	year
Subarctic Zone													
Fairbanks (64°49′ N, 147°52′W)													
K↓	5	34	104	171	223	228	204	142	91	44	10	0	105
T_m	–23.9	–19.4	–12.8	–1.4	8.4	14.7	15.4	12.4	6.4	–3.2	–15.6	–22.1	–3.4
P	23	13	10	6	18	35	47	56	28	22	15	14	287
Sn	35	21	18	7	1	0	0	0	2	24	23	23	153
Cl	6.7	6.4	6.3	6.2	7.0	7.3	7.2	7.7	7.9	8.1	7.0	7.1	7.1
Dir	N	N	N	N	N	SW	SW	N	N	N	N	N	N
u	1.4	1.7	2.1	2.6	3.0	2.9	2.6	2.5	2.5	2.2	1.7	1.3	2.2
Inuvik (68°14′ N, 133°29′ W)													
K↓	2	22	87	181	234	256	216	142	75	27	5	0	104
T_m	–28.6	–27.4	–22.3	–12.7	–0.4	9.6	13.8	10.8	3.6	–7.1	–19.5	–27.3	–8.9
P	12	7	8	8	6	18	32	39	27	24	14	10	206
Sn	12	7	8	8	5	1	0	1	10	23	14	10	99
Cl	3.8	3.7	4.4	4.0	5.9	7.2	7.3	7.2	7.2	6.1	4.3	3.7	5.4
Dir	E	E	E	E	NE	NW	NW	NW	NE	E	E	E	E
u	2	1.9	12.6	3	3.4	3.7	3.4	3.2	3.0	2.6	2.0	2.0	2.7
Churchill (58°45′ N, 94°04′ W)													
K↓	28	69	145	220	247	253	240	183	105	51	28	17	132
T_m	–27.5	–26.4	–19.8	–10.7	–2.3	5.8	12.0	11.6	5.7	–1.1	–11.7	–21.9	–7.2
P	13	14	17	26	30	41	52	61	53	38	39	23	407
Sn	15	14	18	24	18	3	0	0	4	26	42	21	184
Cl	4.3	4.4	5.1	6.2	7.7	7.2	6.4	6.7	8.2	8.2	7.5	5.4	6.4
Dir	NW	NW	NW	NW	N	N	N	NW	N	NW	NW	NW	NW
u	6.3	6.4	6.2	6.5	5.9	5.4	5.5	5.6	6.6	7.2	6.8	7.2	6.3

Table 3 As Table 1 but for the Arctic zone

	J	F	M	A	M	J	J	A	S	O	N	D	year
Arctic Zone													
Barrow (71°18′N, 156°47′ W)													
K↓	0	13	84	187	220	222	182	109	57	24	0	0	92
T_m	–26.8	–27.9	–25.9	–17.7	–7.6	0.6	3.9	3.3	–0.8	–8.6	–18.2	–24.0	–12.4
P	5	4	3	3	3	9	20	23	16	13	6	4	110
Sn	6	5	4	4	4	1	2	2	7	6	9	7	66
Cl	5.3	5.3	5.1	5.9	8.4	8.0	8.2	9.0	9.2	8.7	7.0	5.4	7.1
Dir	SE	NE	NE	E	NE	E	SW	E	NE	NE	NE	NE	NE
u	4.9	5.1	4.9	5.1	5.3	5.1	5.3	5.7	6.1	6.3	5.6	4.9	5.4
Baker Lake (64°18′ N, 96°00′ W)													
K↓	9	37	120	210	260	251	231	158	85	41	15	4	118
T_m	–32.9	–32.8	–26.3	–16.4	–5.8	3.9	10.7	10.0	2.8	–7.5	–20.0	–28.2	–11.9
P	5	4	6	9	8	21	40	45	34	20	9	7	208
Sn	5	4	6	9	5	8	0	0	2	10	9	7	58
Cl	4.5	4.3	4.8	5.5	7.0	7.1	6.5	6.7	7.9	8.0	6.0	4.7	6.1
Dir	NW	NW	NW	N	N	N	N	N	NW	N	N	NW	N
u	6.3	5.5	5.6	6.3	5.4	4.4	4.7	5.4	5.6	6.4	6.0	6.3	5.6
Resolute (74°43′ N, 94°59′ W)													
K↓	0	0	58	175	270	289	225	128	57	15	0	0	102
T_m	–32.6	–33.5	–31.3	–23.1	–10.7	–0.3	4.3	2.7	–4.9	–14.7	–24.2	–28.8	–16.4
P	3	3	3	6	9	13	26	31	18	15	6	5	136
Sn	3	3	3	6	9	7	3	5	15	16	6	5	79
Cl	4.0	4.2	4.1	4.7	7.0	7.6	7.6	8.2	8.4	7.0	4.9	4.0	6.0
Dir	NW	NW	NW	NW	NW	NW	W	SE	N	NW	NW	NW	NW
u	6.0	6.3	6.0	5.5	6.0	6.2	5.6	6.3	7.1	7.0	5.9	5.8	6.1

forest canopies, and blowing snow in tundra areas, enhance sublimation and reduce total snow on the ground at the end of winter. In regions of low precipitation, such as most of the tundra and the drier northern regions of the boreal forest, sublimation limits water availability at the start of the growing season. In dense coniferous canopies, interception can result in up to 40% sublimation, while in open or deciduous forests it may be less than 10% (Pomeroy & Gray 1994). Wind controls snow cover distribution, producing highly variable cover in open tundra and a more uniform distribution in forested areas (Liston & Sturm 1998). Cold, high-latitude snowpacks behave very differently to warm, temperate snowpacks during snowmelt (Marsh 1991; Liston 1995). In temperate areas, ground heat flux is seldom important, with small fluxes from the ground to the snowpack helping to increase melt. In northern permafrost soils, the ground heat flux is from the snow to the ground in spring. This increases the amount of energy required to melt the snowpack and delays melt.

The hydraulic conductivity of permafrost soils is significantly lower than for unfrozen soils, thus limiting groundwater flows. Consequently, the occurrence of permafrost is important in controlling drainage, and therefore the areal extent and spatial distribution of wetlands (Rouse *et al*. 1997; Rouse 2000). The permafrost that underlies Arctic and subarctic regions varies in thickness along temperature, latitudinal and altitudinal gradients. Where the annual mean temperature is higher than –6 °C or the annual mean ground temperature hovers around 0 °C, permafrost is sensitive to warming and may disappear. Warming over a long period would therefore move the permafrost boundaries poleward (Woo *et al*. 1992), reducing the area of permafrost coverage. The most profound physical impact in wetlands would be melting of near-surface ground ice resulting in massive terrain slumping (thermokarst) which would affect all surface features, most prominently in areas of discontinuous permafrost. Ground ice occupies about 70% of the volume of loess soils on the Siberian plains, and warming and thermokarst in this region is causing extensive ecosystem conversion in both tundra and boreal forest (Zimov *et al*. 1997).

In the snow-free season, evaporation and transpiration often exceed precipitation, resulting in a negative water balance (Woo *et al*. 1992). Any increase in the length of the snow-free period or in summer temperatures, would increase evapotranspiration. Unless these changes are accompanied by an increase in precipitation, summer water balances will become increasingly negative (Rouse *et al*. 1992; Rouse 2000), reducing both lake levels and ground water recharge. Thus the impact of environmental change on the water balance depends on the magnitude of changes in both surface temperature and the precipitation regime. Warming of the permafrost can increase liquid water storage, if the water balance is positive, or reduce water storage, if the water balance is negative (Rouse 2000). A large increase in the depth of the active layer would threaten the existence of wetlands. And changes in soil moisture would also strongly affect decomposition and carbon balance (Gorham 1991; Oechel *et al*. 1993).

The flora is more or less in equilibrium with the regional atmospheric and soil climates (e.g. Jacobs *et al*. 1997). Summer temperature, the length of the growing season, and intensity of summer warmth show the greatest correlation with vegetation distribution and species diversity (e.g. Young 1971; Edlund & Alt 1989; Walker 2000). Seasonal snow cover and soil moisture availability also influence the distribution of species and communities. By maintaining a high water table, permafrost can promote anaerobic conditions within rooting zones, restricting the growth of vascular plants, especially trees, and favouring the development of nonvascular plants.

The high latitudes thus present a number of unique features that strongly influence their energy and water balances and their feedback to climate and ecological processes. They also make the system highly sensitive to climate change. The most significant features are the shortness of the growing season, long summer days, permafrost, massive ground ice and cold soils, extensive wetlands and shallow lake systems, open-canopied boreal woodlands and forests, and a nonvascular ground vegetation in both tundra and forest. Because of this ecoclimatic diversity across the circumpolar region, the patterns of energy exchange and climate feedback that are discussed in the following sections exhibit greater variance than in many other biomes.

3 Land–atmosphere energy exchange in northern ecosystems

Solar radiation is the driving force of the Earth's climate. The net radiative forcing at the surface dictates the total amount of energy that is available to be partitioned into secondary surface energy exchanges which, over long time periods, maintain the surface thermal equilibrium. The *radiation-budget* describes the net radiative forcing at the surface (e.g. Oke 1987),

$$Q^* = (K\downarrow - K\uparrow) + (L\downarrow - L\uparrow) \quad (1)$$

This budget represents the balance between the incident ($K\downarrow$) and reflected ($K\uparrow$) visible short-wave radiation, and incoming ($L\downarrow$) and outgoing ($L\uparrow$) long-wave thermal radiation, where Q^* represents the 'net radiation'. Neglecting the typically minor effects of heat storage within canopy air, photosynthetic activity, organic decomposition and geothermal influences, the key surface energy exchange processes that act collectively to dissipate the available net radiation are: sensible (Q_H), latent (Q_E) and ground (Q_G) heat fluxes. This process of energy redistribution is most conveniently summarized by the *surface energy balance* which, in the case of a snow/ice-free surface, is represented as (e.g. Oke 1987)

$$Q^* = Q_H + Q_E + Q_G \tag{2}$$

If the surface is covered with vegetation, then an additional storage term S may appear in (2) to account for energy storage in the canopy if the reference level for Q_G is not identical with the one for Q_H and Q_E. Frequently the need arises to make comparisons between sites and ecosystems that experience different absolute values of Q^*. A less subjective form of the surface energy balance presented in (2) can be obtained by normalizing with respect to the net radiation, resulting in

$$Q_H/Q^* + Q_E/Q^* + Q_G/Q^* = 1 \tag{3}$$

The relative partitions of energy flux at a given site are fairly constant over the diurnal cycle, as has been shown for both the boreal zone (Hurtalová 1997) and the Arctic zone (Eugster *et al*. 1997), although it often varies over the growing season due to changes in weather (Rouse 2000), soil moisture, and stomatal conductance (Baldocchi *et al*. 2000).

3.1 Energy balance studies and data

Recent energy balance data come from long-term studies in the Arctic and boreal zone (e.g. Lafleur & Rouse 1995), intensive field campaigns in the boreal forest of North America (BOREAS, Sellers *et al*. 1997), Scandinavia (NOPEX, Halldin *et al*. 1995; Grelle 1997), and the North American Arctic (ARCSS LAII Flux Study, Weller *et al*. 1995). Additional information comes from Siberian forests (Schulze *et al*. 1995; Arneth *et al*. 1996; Kobak *et al*. 1996; Kelliher *et al*. 1997; Vygodskaya *et al*. 1997; Schulze *et al*. 1999). Most of these studies provide information from single 'representative' sites throughout the growing season for one or more years, although some information is available for short time-periods for replicate sites with a given vegetation type (Eugster *et al*. 1997; Schulze *et al*. 1999). Most early estimates of energy partitioning used the Bowen ratio-energy balance method (Bowen 1926). Many recent studies measure these fluxes directly by eddy covariance (Chahuneau *et al*. 1989). All data available to the authors are tabulated in Table4. Where sufficient long-term data were available, the July mean data were selected. Data from short measuring campaigns during the growing season, and one winter measurement that has been published were also included. To provide a clearer understanding of the potential seasonal and climatic influences on the surface radiation-budget, the following sections describe the typical behaviour, and variations in, the individual components of (1), using the data set in Table 4.

3.2 Solar radiation

After the long winter, the solar input in the high latitudes quickly reaches levels in May that exceed the solar input in the mid-latitudes. While Arctic tundra is exposed to 24 h of daylight over the summer months, the boreal forest zone generally experiences a short period of darkness or dusk, depending on latitude. The daily maximum and amplitude of incoming solar radiation is greatest at the southern extreme of the boreal zone and decreases with increasing latitude. The daily total of solar energy received at the surface in summer is, however, more strongly determined by length of day than by the daily maximum or amplitude (Fig. 1). A summertime local minimum of mean daily global radiation is therefore found in the northern boreal or southern Arctic zone (Fig. 1). In June this minimum ranges from 200 to 225 W m^{-2} in the far north of western and central Siberia, and the eastern Hudson Bay region. Values are higher near the Arctic circle in Alaska and central Canada (225–250 W m^{-2}), and near the Arctic circle in eastern Siberia (250–275 W m^{-2}).

The maximum high-latitude radiation occurs over Greenland where the June average exceeds 350 W m^{-2} (Fig. 1). This is due to the Greenland ice sheet, over which atmospheric transmission is extremely high because of the low atmospheric moisture over permanent ice at a high altitude. Over surfaces that are free of snow and ice, mean daily global radiation is well below 300 W m^{-2} (Fig. 1). This observed uneven distribution of solar radiation over the northern hemisphere also leads to regional differences in the surface energy balance at identical northern latitudes.

Net short-wave radiation at the surface: the effect of albedo. A considerable fraction of the solar radiation which passes through the atmosphere to the surface is reflected directly back into space. The proportion of incident radiation which is reflected from the surface varies diurnally and seasonally as a function of the reflectivity and roughness of the surface, and solar elevation angle. The difference between the incident and reflected radiation is termed the net short-wave radiation, $K^* = K\downarrow - K\uparrow$. The ratio of reflected to incident radiation is referred to as the albedo $\alpha = K\uparrow/K\downarrow$ where actual albedo $\alpha \geqslant \alpha_{min}$. Typically, the minimum albedo value for a surface occurs shortly before

Table 4 Characteristic surface energy exchange parameters for Arctic tundra and boreal forest ecosystems compiled from various published and unpublished data sources

Code	Vegetation type	Locality	Time period	Reference	Area 10^6 km^2	K↓ W m^{-2}	Q^* W m^{-2}	T_m °C	Q_E/Q^*	Q_H/Q^*	Q_G/Q^*	$Q_{E,max}$ W m^{-2}	$Q_{H,max}$ W m^{-2}	Q_E/$Q_{E,eq}$	$G_{s,\ max}$ mm s^{-1}	Q^*=a intercept	+b K↓ slope	albedo min.	TDD deg. days	Method (site ID)
1	2	3	4	5	6	7	8	9	10	11	12	13	14	15	16	17	18	19	20	21
L	**TUNDRA**, low arctic				9.0															
	lakes				*no data*															
Lls	shallow																			
	deep																			
Lld1	Toolik lake Toolik Field Station, Alaska, USA	68.6°N 149.6°N	208-212 1995	R01		230	126	10.1*	0.10	0.08	0.82	61	54	1.07		-53.5	0.803	0.05	473[el] (R02)	ECEB$_3$ (95-Tl)
	shrub				*2.0*															
Ls1	riparian (willow shrubs on sandy soil) Sagavanirktok River valley, Alaska, USA	69.1°N 148.8°W	191-198 1995	R03		240	134	17.1*	0.70	0.25	0.05	293	185	1.00	9.0	-21.6	0.652	0.15[c]	552[l] (R02)	EC (95-9)
Ls2	riparian (high LAI in bottom of creek, dry warm air advection) May creek, Alaska, USA	68.6°N 150.6°W	201-210 1996	R01		214	95	12.7*	0.72	0.21	0.07	369	99	1.47	13.7	-36.2	0.618	0.15 [c]	440 (R02)	EC (96-16)
Ls3	shrub tundra (watertrack) Happy Valley, Alaska, USA	69.1°N 149.0°W	177-180 1994	R04		239	132	7.9*	0.33	0.48	0.10	140	285	0.64	6.7	-33.3	0.67	0.16 [c]		EC (94-1)
Ls4	watertrack (Betula nana and Salix sp.) near Happy Valley, Alaska, USA	69.1°N 148.6°W	191-199 1995	R03		206	103	15.1*	0.48	0.31	0.21	234	207	0.82	6.5	-31.0	0.644	0.16 [c]	499[l] (R02)	EC (95-10)
Ls5	alder steppe Ice Cut, Alaska, USA	69.0°N 148.8°W	192-200 1996	R01		193	76	13.3*	0.55	0.33	0.12	235	188	0.94	10.8	-46.7	0.636	0.145 [c]	569 (R02)	EC (96-13)
Ls6	shrub tundra (shrubs intermixed with tussocks, dry warm air advection) May creek, Alaska, USA	68.6°N 150.6°W	201-208 1996	R01		222	76	14.9*	0.44	0.46	0.11	270	163	1.51	6.6	-42.1	0.614	0.155 [c]	442 (R02)	EC (96-15)
	non-shrub, coastal				*1.2*															
Lc1	coastal tundra (mixture of lakes and wet polygonal tundra) Prudhoe Bay, Alaska, USA	70.3°N 148.9°W	196-209 1994/95	R05				5.5[g]	0.35	0.50	0.15								322[l] (R02, 1995)	EC

Code	Vegetation type	Locality	Time period	Reference	Area 10^6 km^2	K↓ W m^{-2}	Q^* W m^{-2}	T_m °C	Q_E/Q^*	Q_H/Q^*	Q_G/Q^*	$Q_{E,max}$ W m^{-2}	$Q_{H,max}$ W m^{-2}	$Q_E/Q_{E,eq}$	$G_{s,\ max}$ mm s^{-1}	$Q^*=a$ intercept	$+b$ K↓ slope	albedo min.	TDD deg. days	Method (site ID)
1	2	3	4	5	6	7	8	9	10	11	12	13	14	15	16	17	18	19	20	21
Lc2	coastal tundra (moist polygonal tundra) Prudhoe Bay, Alaska, USA	70.3°N 148.9°W	182-190 1995	R01		224	113	10.6*	0.26	0.55	0.19	141	237	0.65	5.6	-30.0	0.619	0.175 [c]	322[l] (R02)	EC (95-1)
Lc3	coastal tundra (wet polygonal tundra) Prudhoe Bay, Alaska, USA	70.3°N 148.9°W	182-189 1995	R01		244	128	9.8*	0.40	0.44	0.16	219	220	0.84	8.7	-36.2	0.675	0.175 [c]	343[l] (R02)	EC (95-2)
Lc4	coastal tundra (offshore winds) Prudhoe Bay, Alaska, USA	70.3°N 148.9°W	208 1994	R06		274	139	16.9*	0.39	0.22	0.32									EC
Lc5	coastal tundra (onshore winds)	70.3°N 148.9°W	209 1994	R06		273	153	9.5*	0.32	0.50	0.13									EC
	non-shrub, non-coastal wet				*no data*															
Lw1	wet meadow (sedges) Happy Valley, Alaska, USA	69.2°N 148.9°W	209-211 1994	R04		296	154	15.9*	0.52	0.14	0.14	196	82	0.86	6.8	-51.1	0.7	0.175 [c]		EC (94-5)
Lw2	wet fen Imnavait Creek, Alaska, USA	68.6°N 149.6°W	216-224 1995	R01		154	66	4.1*	0.67	0.26	0.07	232	129	1.10	13.1	-28.6	0.619	0.175 [c]	422[el] (R02)	EC (95-7)
	non-shrub, upland moist				*1.9*															
Lu1	upland non-acidic Sagwon Hills, Alaska, USA	69.4°N 148.7°W	170-180 1995	R03		217	101	7.9*	0.43	0.41	0.16	199	220	1.08	10.4	-37.3	0.633	0.147	505[l] (R02)	EC (95-3)
Lu2	upland acidic (typical tussock tundra) Sagwon Hills, Alaska, USA	69.4°N 148.8°W	172-181 1995	R03		242	121	10.1*	0.49	0.40	0.11	256	231	0.85	6.6	-45.6	0.677	0.155	492[l] (R02)	EC (95-4)
Lu3	upland acidic (moist tussock tundra) Happy Valley, Alaska, USA	69.1°N 148.8°W	July 1994/95	R07			244	10.7[g]	0.48	0.38	0.14				8.0				883	EC
Lu4	upland tundra (30% dry upland, 62% moist, 4% lake) Bethel, Alaska, USA	60.8°N 161.8°W	195-225 1988	R08					0.40	0.40	0.20							0.19		EC
Lu5	tussock tundra (upland acidic tussock tundra) Happy Valley, Alaska, USA	69.1°N 149.0°W	180-184 1994	R04		338	166	12.8*	0.42	0.35	0.24	212	179	0.73	5.7	-56.9	0.66	0.155 [c]		EC (94-2)
Lu6	tussock-shrub tundra (acidic tussock tundra, some shrubs) Happy Valley, Alaska, USA	69.1°N 149.0°W	184-189 1994	R04		251	132	10.7*	0.38	0.35	0.13	172	186	0.80	6.5	-18.6	0.63	0.155 [c]		EC (94-3)

Code	Vegetation type	Locality	Time period	Reference	Area 10^6 km^2	K↓ $W\ m^{-2}$	Q^* $W\ m^{-2}$	T_m °C	Q_E/Q^*	Q_H/Q^*	Q_G/Q^*	$Q_{E,max}$ $W\ m^{-2}$	$Q_{H,max}$ $W\ m^{-2}$	$Q_E/Q_{E,eq}$	$G_{s,\ max}$ $mm\ s^{-1}$	$Q^*=a$ intercept	$+b$ K↓ slope	albedo min.	TDD deg. days	Method (site ID)
1	2	3	4	5	6	7	8	9	10	11	12	13	14	15	16	17	18	19	20	21
Lu7	tussock tundra (upland acidic tussock tundra) Toolik Lake, Alaska, USA	68.1°N 149.6°W	214-219 1994	R04		242	110	18.3*	0.40	0.22	0.17	121	120	0.62	2.3	-28.5	0.64	0.155 [c]		EC (94-6)
Lu8	tussock tundra (upland acidic tussock tundra) Toolik Lake, Alaska, USA	68.6°N 149.6°W	200-213 1995	R01		156	79	6.9*	0.46	0.42	0.12	280	191	0.89	13.3	-22.5	0.655	0.155 [c]	476[l] (R02)	EC (95-6)
Lu9	upland tundra (acidic tussock tundra on slope) Imnavait Creek, Alaska, USA	68.6°N 149.6°W	219-226 1995	R01		173	73	11.1*	0.55	0.25	0.20	192	213	0.93	6.7	-38.7	0.638	0.155 [c]	423[el] (R02)	EC (95-8)
Lu10	upland tundra (acidic tussock tundra on slope) Ice Cut, Alaska, USA	69.0°N 148.8°W	192-200 1996	R01		194	84	13.2*	0.61	0.27	0.12	277	204	0.99	12.2	-34	0.617	0.155 [c]	564 (R02)	EC (96-14)
	non-shrub, upland dry/mesic				*1.4*															
Ld1	upland heath (heath on moist soil) Toolik Field Station, Alaska, USA	68.6°N 149.6°W	184-190 1996	R01		188	85	12.7*	0.50	0.38	0.12	239	218	0.77	5.6	-43.9	0.641	0.155	470 (R02)	EC (96-hA)
Ld2	dry heath ridge (top of ridge position) Sagwon Hills, Alaska, USA	69.4°N 148.9°W	196-208 1994	R04		298	120	17.5*	0.29	0.44	0.15	94	198	0.54	2.3	-25.6	0.59	0.16 [c]		EC (94-4)
Ld3	mountain barrens Imnavait mountain top, Alaska, USA	68.8°N 149.4°W	200-207 1995	R01		202	70	3.0*	0.96	0.64	-0.60	160	129	0.87	24.4	-16.6	0.654	0.10 [c]	385[l] (R02)	$ECEB_1$ (95-5)
H	**TUNDRA**, high arctic																			
	coastal wet tundra				*no data*															
Hc1	wet sedge tundra Barrow, Alaska, USA	71.3°N 156.8°W	July 1957/58 1973/74	R09[a]		206	130	10.0[m]	0.50	0.45	0.05							0.10	926	AERO
Hc2	wet sedge coastal (dry conditions, onshore winds) Barrow Alaska, USA	71.3°N 156.8°W	200-214 1993	R10, R11		250	139	7.3[m]	0.24	0.61	0.15							0.17		EC
Hc3	wet sedge coastal (dry conditions, offshore winds) Barrow, Alaska, USA	71.3°N 156.8°W	200-214 1993	R10, R11		250	139	7.3[m]	0.45	0.38	0.17							0.17		EC

Code	Vegetation type	Locality	Time period	Reference	Area 10^6 km^2	K↓ W m^{-2}	Q^* W m^{-2}	T_m °C	Q_E/Q^*	Q_H/Q^*	Q_G/Q^*	$Q_{E,max}$ W m^{-2}	$Q_{H,max}$ W m^{-2}	$Q_E/Q_{E,eq}$	$G_{s,\ max}$ mm s^{-1}	$Q^*=a$ intercept	$+b$ K↓ slope	albedo min.	TDD deg. days	Method (site ID)
1	2	3	4	5	6	7	8	9	10	11	12	13	14	15	16	17	18	19	20	21
Hc4	wet sedge coastal (standing water, all wind directions) Barrow, Alaska, USA	71.3°N 156.8°W	200-214 1993	R10, R11		250	139	7.3^m	0.45	0.40	0.15							0.17		EC
	lakes				*no data*															
	shallow																			
	deep																			
	semidesert				*2.4*															
Hu1	upland tundra heath Axel Heiberg Island, NWT, Canada	79.3°N 90.5°W	July 1969/70	R09		229	179	5.8* 5.5^m	0.47	0.37	0.16							0.22	593	BREB
Hu2	upland tundra heath Axel Heiberg Island, McGill Research Stn., Canada	79.3°N 90.5°W	July 1969/70	R12			111		0.47	0.38	0.15							0.10		BREB
Hu3	upland tundra heath Axel Heiberg Island, McGill Research Stn., Canada	79.3°N 90.5°W	August 1969/70	R12			69		0.58	0.30	0.12							0.10		BREB
Hu4	upland tundra heath Svalbard, Norway	79.6°N 13.0°E	summer 1990	R13		185	85	7.2*	0.60	0.27	0.13	105	80			-20	0.627	0.16		BREB
Hu5	upland tundra heath Svalbard, Norway	79.6°N 13.0°E	July 1990/91	R13		200	110	5.4*												???
Hu6	Luzula lichen heath Svalbard, Norway	78.9°N 11.9°E	July 1995	R14			104	6.4*	0.45	0.35	0.20							0.08		ECEB$_2$
Hu7	dry tundra (80% dry sedges and dwarf shrubs, 20% bare soil and gravel) Sisimiut, Greenland	67.1°N 50.3°W	140-165 1988	R15		253	131	4.5*	0.37	0.53	0.10	100	200					0.16		BREB
	polar barrens				*no data*															

Code	Vegetation type	Locality	Time period	Refer-ence	Area 10^6 km^2	K↓ W m^{-2}	Q^* W m^{-2}	T_m °C	Q_E/Q^*	Q_H/Q^*	Q_G/Q^*	$Q_{E,max}$ W m^{-2}	$Q_{H,max}$ W m^{-2}	$Q_E/Q_{E,eq}$	$G_{s,\,max}$ mm s^{-1}	$Q^*=a$ inter-cept	$+b$ K↓ slope	albedo min.	TDD deg. days	Method (site ID)
1	2	3	4	5	6	7	8	9	10	11	12	13	14	15	16	17	18	19	20	21
B	**BOREAL FOREST**				21.8															
	non-vegetated																			
	lakes				*no data*															
Bls1	shallow Churchill, Manitoba, Canada	58.7°N 94.3°W	July 1991	R16		235	163	14.9* 12.0^m	0.85	0.11	0.04					-3.8	0.61	0.06	1083	BREB
Bld1	deep Great Slave Lake, Canada	61.9°N 113.7°W	205-212 213-243 244-253	R17		263 189 156	159 100 77		0.41 0.57 0.26	0.01 0.09 -0.06	0.58 0.34 0.80									EC-Cal
	urban barrens																			
Bu1	upland heath (lichen-sedge on gravelly soil)	58.7°N 94.3°W	July 1991	R16		235	128	14.9* 12.0^m	0.50	0.30	0.20					-3.9	0.61	0.15	1083	BREB
	vegetated																			
	non-closed canopy																			
Bs1	treeline shrub tundra shrub tundra, Churchill, Manitoba, Canada	58.7°N 94.3°W	152-243 1989/90	R18	*no data*		125	9.7^g	0.60	0.28	0.12							0.13		BREB
Bs2	treeline shrub tundra (Betula glandulosa tussock tundra) Wiseman, Alaska, USA	67.5°N 150.1°N	216-225 1996	R01	*no data*	172	76	8.3*	0.65	0.30	0.05	375	189	1.17	15.6	-28.1	0.606	0.145		EC (96-18)
Bs3	treeline shrub tundra Sayan Mountain Range, Russia	53.5°N 95.0°E	mid- summer, 2 years	R19					0.48	0.48	0.04									
	forest tundra				*0.8*															
Bft1	open subarctic, wet (on peat; spruce and larch vegetation) Churchill, Manitoba, Canada	58.7°N 94.3°W	152-243 1989/90	R18			129	9.7^g	0.53	0.38	0.09							0.12		BREB
Bft2	open subarctic, wet (on peat; spruce and larch vegetation) Churchill, Manitoba, Canada	58.7°N 94.3°W	July 1991	R20	235	139	14.9* 12.0^m	0.65	0.26	0.09			0.83	11.1	–12.3	0.64	0.16	1083	BREB	

Code 1	Vegetation type 2	Locality 3	Time period 4	Refer-ence 5	Area 10^6 km^2 6	K↓ W m^{-2} 7	Q^* W m^{-2} 8	T_m °C 9	Q_E/ Q^* 10	Q_H/ Q^* 11	Q_G/ Q^* 12	$Q_{E,max}$ W m^{-2} 13	$Q_{H,max}$ W m^{-2} 14	Q_E/ $Q_{E,eq}$ 15	$G_{s,\ max}$ mm s^{-1} 16	Q^*=a inter-cept 17	+b K↓ slope 18	albedo min. 19	TDD deg. days 20	Method (site ID) 21
Bft3	treeline forest (Picea mariana) Wiseman, Alaska, USA	67.5°N 150.1°N	216-225 1996	R01		154	93	8.7*	0.49	0.45	0.06	245	315	0.83	9.4	-21.7	0.741	0.125 [x]		EC (96-17)
Bft4	subarctic lichen woodland Shefferville, Quebec, Canada	54.9°N 66.7°W	1990	R40				13.2* 12.5^m	0.35	0.58	0.07									EC
	early successional				*0.7*															
Bfr1	logged 12-yr regenerating forest (Pinus sylvestris), Zotino, Siberia	61°N 89°E	06-26 July 1996	R39			303	23.8	0.18	0.52	0.30	239	342							$ECEB_2$
Bfr2	logged 6-yr regenerating forest (Pinus sylvestris)	60.7°N 89.4°E	186-206 1996	R43		268	136	24.3	0.17	0.63	0.14	166	364			–44.1	0.67			EC
	post-fire / post-insect				*no data*															
	agriculture				*no data*															
	mires (fens, bogs, ...)				*no data*															
Bw1	fen (hummocky sedge fen on peat wetland) Churchill, Manitoba, Canada	58.7°N 94.3°W	July 1991	R21		235	138	14.9* 12.0^m	0.73	0.18	0.09					-3.9	0.61	0.12	1083	BREB
Bw2	bog Central Siberia		summer 1996	R38										1.05	14.1					$ECEB_2$
Bw3	bog (Sphagnum spp.) Zotino, Siberia, Russia	61°N 89°E	10-16 July 1996	R39			231	19.5	0.53	0.31	0.16									$ECEB_2$
Bw4	peat bog Hudson Bay lowlands, Canada	51.5°N 81.8°W	25 June- 28 July 1990	R41				16.1	0.46	0.34	0.10			0.63 0.75		-22	0.64			EC BREB
Bw5	fen Shefferville, Quebec, Canada	54.9°N 66.7°W	1990	R42					0.63	0.25	0.12							0.11		$ECEB_1$
	closed canopy																			
	evergreen forests																			
	coniferous: spruce, fir & mixed (dark taiga)				*13.2*															
Bfc1	Black spruce (Picea mariana) Prince Albert, Saskatchewan, Canada	53.9°N 105.1°W		R22			143		0.42	0.47	0.09			0.74	4.4			0.11 (R23)		EC

Code	Vegetation type	Locality	Time period	Reference	Area 10^6 km^2	K↓ W m^{-2}	Q^* W m^{-2}	T_m °C	Q_E/Q^*	Q_H/Q^*	Q_G/Q^*	$Q_{E,max}$ W m^{-2}	$Q_{H,max}$ W m^{-2}	$Q_E/Q_{E,eq}$	$G_{s,\,max}$ mm s^{-1}	$Q^*=a$ intercept	$+b$ K↓ slope	albedo min.	TDD deg. days	Method (site ID)
1	2	3	4	5	6	7	8	9	10	11	12	13	14	15	16	17	18	19	20	21
Bfc2	Black spruce (Picea mariana) Prince Albert, Saskatchewan, Canada	53.9°N 105.1°W	IFC1 IFC2 IFC3	R24					0.38 0.45 0.37	0.58 0.53 0.53								0.11 (R23)		EC
Bfc3	P. sylvestris, P. abies Norunda, Sweden	60.5°N 17.3°E	July 1995	R32			144		0.54	0.43	0.03									EC
Bfc4	P. sylvestris, P. abies Flakaliden, Sweden	64.1°N 19.5°E	July 1996	R32			66		0.55	0.41	0.02									EC
	coniferous: pine (light taiga)				*0.9*															
Bfp1	Jack pine (Pinus banksiana) Nipawin, Saskatchewan, Canada	53.9°N 104.7°W	143-162 1993	R25, R26			121		0.38	0.48	0.01			0.38	0.8	-27.4 (R25)	0.893 (R25)	0.086 (R23)		EC
Bfp2	Jack pine (Pinus banksiana) (75% cover) Lac du Bonnet, Manitoba, Canada	50.3°N 95.9°W	117-277 1985	R27					0.34	0.60	0.06							0.086 (R23)		$ECEB_2$
Bfp3	Jack pine (Pinus banksiana)	55.9°N 98.6°W	200-230 1994	R28		194	107	16.2	0.23	0.52	0.10	100	280		5.0	-41.0	0.76	0.091	1810	EC
Bfp4	Jack pine WINTER (Pinus banksiana) Prince Albert National Park	53.9°N 106.1°W	62, 63, 77, 78 1994	R29			28		1.27	0.75	-1.02							0.12		EC
Bfp5	Scots pine (Pinus sylvestris) Jadraås, Sweden	60°N 16°E	149-165 1990	R30			196		0.17	0.64	0.19									EC
Bfp6	Pine forest (Pinus sylvestris) Zotino, Russia	61°N 89°E	190-207 1996	R31			166		0.38	0.66	-0.04			0.60	2.3					$ECEB_2$
Bfp7	Pinus sylvestris Central Siberia		summer 1996	R38										0.23	1.8					EC
	deciduous forests																			
	broadleafed				*2.9*															
Bfd1	Aspen/hazel (Populus tremuloides) Prince Albert, Sask. Canada	53.7°N 106.2°W	209-220 1994	R33, R34			124		0.68	0.14	0.18			0.99	19.2			0.156 (R23)		EC

Code	Vegetation type	Locality	Time period	Reference	Area 10^6 km^2	K↓ W m^{-2}	Q^* W m^{-2}	T_m °C	Q_E/Q^*	Q_H/Q^*	Q_G/Q^*	$Q_{E,max}$ W m^{-2}	$Q_{H,max}$ W m^{-2}	$Q_E/Q_{E,eq}$	$G_{s,\,max}$ mm s^{-1}	Q^*=*a* intercept	+*b* K↓ slope	albedo min.	TDD deg. days	Method (site ID)
1	2	3	4	5	6	7	8	9	10	11	12	13	14	15	16	17	18	19	20	21
Bfd2	Willow/birch (shrub forest on peat) Churchill, Manitoba, Canada	58.7°N 94.3°W	July 1991	R35		235	140	14.9* 12.0[m]	0.68	0.19	0.14							0.16	1083	BREB
Bfd3	Aspen/willow (Populus tremuloides, Salix spp.) Lac du Bonnet, Manitoba, Canada	50.3°N 95.9°W	117-277 1985	R27					0.58	0.40	0.02							0.156 (R23)		$ECEB_2$
Bfd4	Aspen/hazel (Populus tremuloides) Prince Albert, Sask. Canada	53.7°N 106.2°W	pre-leaf	R36					0.10	0.73	0.09							0.156 (R23)		EC
			full-leaf						0.61	0.25	0.03			0.91	12.0					
	larch (light taiga)				3.2															
Bfl1	Larch forest	61°N	21 July	R37			248		0.25	0.44	0.31			0.52	5.0					$ECEB_2$
	(Larix gmelinii) Yakutsk, Siberia, Russia	128°E	14-17 Jul. 1993	R37			143		0.37	0.47	0.16									$ECEB_2$
Bfl2	Larch forest (Larix gmelinii) Siberia, Russia	61°N 128°E	1993	R38										0.60	2.3					EC
	WATER SURFACES Arctic tundra and boreal forest				1.8															
	SNOW and ICE Arctic tundra and boreal forest				2.6															
	TOTAL AREA				35.2															

[a]data cited in given reference; *mean July temperature during measuring period; [m]mean July temperature; [g]mean growing season temperature (1 June–31 August); [w]mean January temperature; [e]partially extrapolated due to data gaps; [l]low estimate due to incomplete coverage of growing season (23 June–11 August 1995); [c]data point was measured at a different location over comparable ecosystem/surface type; [x]data point measured at site Bs2 and then decreased by 0.02.

BREB, Bowen-Ratio Energy Balance method.

AERO, Aerodynamic gradient method.

EC, Eddy covariance method for Q_H and Q_E; Q_G measured with soil heat flux plates and soil temperature probes (to correct for heat storage above heat flux plates).

ECEB, $ECEB_1$: Eddy covariance method for Q_H, Q_E estimated from energy balance closure ($Q_E = Q^* – Q_G – Q_H$).

$ECEB_2$: eddy covariance for Q_H and Q_E, Q_G estimated from energy balance closure ($G = Q^* – Q_H – Q_E$).

$ECEB_3$: eddy covariance method for Q_H, Q_E estimated from gradient measurement and Kh derived from Q_H and $\Delta T/\Delta z$, Q_G estimated from energy balance closure ($Q_G = Q^* – Q_H – Q_E$).

EC-Cal, Eddy covariance method for Q_H and Q_E; Q_G estimated using calorimetric method based on temperature profiles in the lake.

Description of column contents 1 Internal classification code used for reference in text and figures. 2 Ecosystem type. 3 Locality of measuring site in geographical coordinates (latitude and longitude). 4 Time period covered by measurements, day of year and year (e.g. 191–198 1995) or month and years (only for long-term sites where selection of monthly data from several years was possible).
5 Reference for data (see below). The References generally point to a description of the site and data set. 6 Area estimates are for circumpolar land regions (oceans excluded) north of 40°N, but excluding coastal forest, grasslands/crops, and desert in the south (i.e. areas of nonboreal or tundra vegetation). Data are based on preliminary 1-km AVHRR vegetation classification of the Arctic (Jan 1998), by M. Fleming, USGS/EROS Field Office and UC Berkeley. 7 Average global radiation during the month of July (where applicable) or during the measuring period given in column 4. 8 Average net radiation during the month of July (where applicable) or during the measuring period given in column 4. 9 Average air temperature during the month of July (where applicable) or during the measuring period given in column 4. See 10–12 footnotes above. Energy partitioning values for Q_E/Q^*, Q_H/Q^*, and Q_G/Q^*, respectively (derived from daily flux averages). 13 Maximum hourly Q_E measured during the time period given in column 4. 14 Maximum hourly Q_H measured during the time period given in column 4. 15 Priestley–Taylor α_{PT} (ratio of actual evapotranspiration Q_E to equilibrium evaporation $Q_{E,eq}$). 16 Maximum canopy conductivity $G_{s,max}$ for daytime conditions (typically determined from the data obtained during the 6 h centred at local noon). This value was derived by solving the Penman-Monteith equation (e.g. Jarvis & McNaughton 1986) for G_s. 17–18 Intercept Q^* and slope b of the regression of net radiation Q^* as a function of global radiation K↓. 19 Minimum daytime albedo during overcast conditions, or average daytime albedo (estimated from Betts & Ball 1997) where minimum daytime albedo was not available. 20 Thawing degree days (sum of all days with air temperatures above 0 °C, times the average daily temperature in°C). 21 Measuring method used for energy budget components measured, and project-specific site identification (in brackets).

References and additional experimental details Remark: leaf area index (LAI) is one-sided green leaf area of vascular plants per unit of ground area.
R01: W. Eugster and F. S. Chapin, III, unpublished data. Measuring equipment and accuracy is found in reference R03 (below). All sites that were not included in R03 are referenced here with R01. Ground heat flux was derived from four heat flux plates and soil temperature sensors that measured the average temperature of the soil layer on top of the heat flux plates. Soil heat capacity (volumetric contents of mineral soil, organic matter, and water) was measured at the end of the measuring period for the exact soil slabs where the ground heat flux measurements were performed. Q_G was derived by area-weighted averaging of the four measurements at each site according to a microsite classification obtained by D. A. Walker (pers. comm.). R02: Nelson *et al.* (1997), and R02[a]: additional data prepared by Kolja Shiklomanov (pers. comm.). R03: Eugster *et al.* (1997) and Walker *et al.* (1998). Details identical to R01. R04: McFadden *et al.* (1998). R05: Vourlitis & Oechel (1997). R06: Harazono *et al.* (1996). R07: Vourlitis & Oechel (1998). The data displayed in Fig. 8(f) were extracted from the NSIDC database (July data of 1994 and 1995). R08: Fitzjarrald & Moore (1992). R09: Ohmura (1981). R09[a]: data were compiled from Thornthwaite (1957, 1958), Maykut & Church (1973), and Weller & Holmgren (1974). R10: Yoshimoto *et al.* (1996). R11: Harazono *et al.* (1995). R12: Ohmura (1984). R13: Scherer (1992), and Scherer *et al.* (1993). Vegetation description after Thannheiser (1992): *Salix polaris-Drepanocladus uncinatus* community ('Schneebodenvegetation'). Data from 14 July to 23 August 1990. Slope and intercept of $Q^* = a + b$K↓ regression estimated from their Fig. 3; $Q_{H,max}$ and $Q_{E,max}$ estimated from their Fig. 8; albedo estimated from their Fig. 2. R14: Harding & Lloyd (1998). Values determined from their Fig. 2(a) (temperature) and Fig. 7(a) for 1–31 July 1995. R15: Rott & Obleitner (1992). $Q_{E,max}$ and $Q_{H,max}$ estimated from figures in the paper. Observation period: 19 May to 13 June 1988. R16: Boudreau & Rouse (1995). Shallow subarctic lake, about 1 m deep and 1 km in diameter. R17: Dr P. Blanken, pers. comm. to W. R. Rouse. Location: near centre of Great Slave Lake. Depth of water: 60 m. Lake storage is determined calorimetrically from temperature profiles. Q_E employs eddy correlation. R18: Lafleur *et al.* (1992). R19: Tchebakova *et al.* (1992), communicated by E. Vaganov. R20: Lafleur & Rouse (1995). R21: Rouse (1998). R22: Jarvis *et al.* (1997). Canopy height: 11 m, LAI = 4.5. R23: Betts & Ball (1997). R24: Pattey *et al.* (1997). Same site as Bfc1. R25: Baldocchi & Vogel (1996). Canopy height: 13.5 m; LAI = 1.9–2.2. Data are bin averaged by time for 19-day periods from Julian day 143–162. R26: Baldocchi *et al.* (1997). R27: Amiro & Wuschke (1987). Jack pine forest site: upland, sparse *Pinus banksiana* canopy and rock outcrops cover about 75% of its area; aspen/willow forest site: flat, low-lying region vegetated by *Salix* spp. and *Populus tremuloides*. R28: D. R. Fitzjarrald and K. E. Moore, unpubl. data, pers. comm. to J. P. McFadden. R29: Harding & Pomeroy (1996). Height: 16–22 m. R30: Dennis D. Baldocchi and Christer Johansson, unpubli. data. Tree age: 135 years. Stand density: 350 trees ha^{-1}. Understorey: *Calluna vulgaris*, *Vaccinium vitis-idaea* and *Cladonia rangifera*. LAI = 3.3. R31: Kelliher *et al.* (1998). Tree age: 215 years. Average tree height: 16 m. Tree density: 290 ha^{-1}, tree LAI: 1.5, lichen surface area index: 6.0. R32: Grelle (1997). R33: Black *et al.* (1996). R34: Bonan & Davis (1997). Canopy height: 21 m; LAI = 5.1 (1.8 aspen plus 3.3 hazel understorey). Averaged by hour for days 209–220 1994. R35: Blanken & Rouse (1995). R36: Blanken *et al.* (1997). LAI = 5.6. Storage term (not included in Table 4): 0.08 Q^* (preleaf) and 0.11 (full-leaf), respectively. R37: Kelliher *et al.* (1997), Hollinger *et al.* (1998). Canopy height: 12 m. LAI = 1.5. Tree density: 1750 ha^{-1}. Understorey: *Vaccinium*, *Arctostaphylos*. Soil: inceptisol, pergelic cryochrept. R38: Valentini *et al.* (1999a). Values extracted from their table. R39: Valentini *et al.* (1999b). 12-yr-old regenerating forest: LAI = 0.2; canopy height: 2.5 m; tree density: 1700 ha^{-1}. R40: Fitzjarrald & Moore (1994). Tree density: 616 ha^{-1}. Tree composition: 79% black spruce, 6% white spruce, 13% tamarack, 2% mountain alder. Average height of spruce: 6.5 m. Understorey: lichen (*Cladonia* sp.) with scattered Labrador tea (*Ledum groenlandicum*). Adjusted values are reported in this table. R41: den Hartog *et al.* (1994). 9–23% water cover; 19–28% lichen and *Sphagnum* mosses. R42: Moore *et al.* (1994). On discontinuous permafrost. R43: Rebmann *et al.* (Submitted). Canopy height: 1m; LA1 = 0.2.

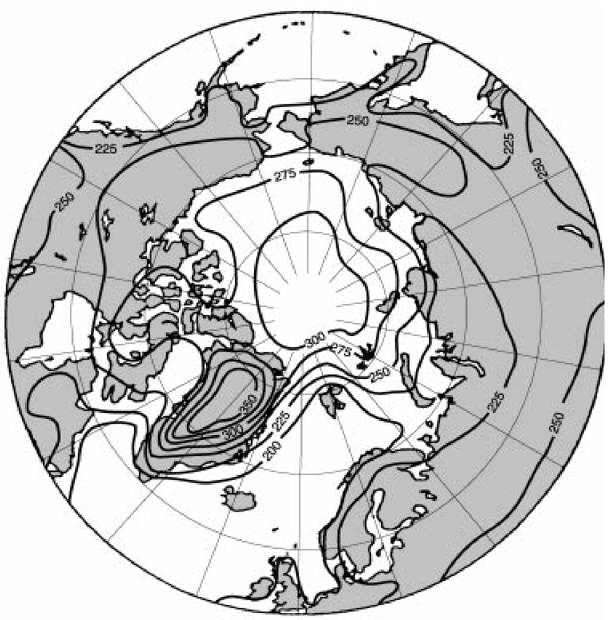

Fig. 1 Monthly mean global radiation for the northern hemisphere north of 50°N during June. Units in W m^{-2} (redrawn from Ohmura & Gilgen 1993b; copyright by the American Geophysical Union).

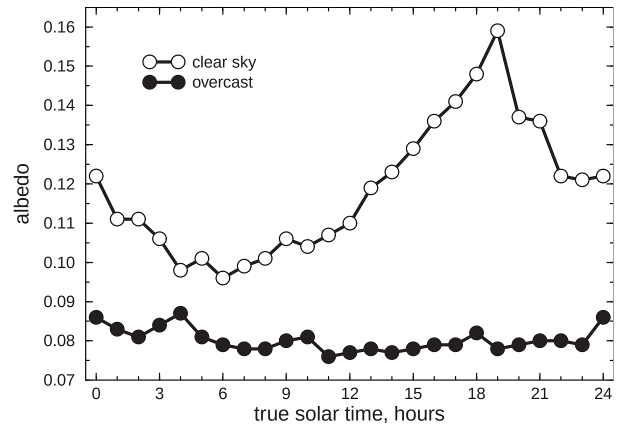

Fig. 2 Diurnal course of short-wave albedo over bare tundra on Axel Heiberg Island during 14 selected days with (a) clear sky or trace clouds (open symbols) and (b) overcast conditions (filled symbols). Minimum albedo is at 06.00 hours true solar time during clear sky conditions ($\alpha = 0.096$) and at 11.00 hours with overcast sky ($\alpha = 0.076$). Data from Ohmura (1981).

solar noon and increases with decreasing solar elevation angle. In GCMs the diurnal course of α is typically described empirically (e.g. a quadratic polynomial fit, Fennessy & Xue 1997), or by a simple linear regression between α and $K\downarrow$ (Betts & Ball 1997).

Effects of clouds on albedo. Under clear-sky conditions, the timing of minimum albedo reflects both sun angle and the diurnal course of soil moisture (Ohmura 1981). As the soil dries during the day, the albedo increases under clear sky conditions. This effect is less pronounced in vegetated tundra or boreal forest, where changes in the wetness of plant leaves and leaf angle relative to the sun influence the diurnal course of albedo, but soil moisture has negligible influence.

Clouds reduce minimum albedo by roughly 0.02 in both vegetated and unvegetated tundra, due to the better penetration of diffuse light into the plant canopy and soil (Fig. 2). The minimum albedo, either measured or estimated over some northern ecosystems during overcast conditions, is presented in Table 4 for modelling purposes. Because few studies specify the difference between clear-sky albedo and albedo during overcast conditions, it is suggested that the tabulated minimum albedo (Table 4) be increased by 0.02 for modelling clear-sky conditions, if no better information is available.

Seasonal changes in albedo. Seasonal albedo changes are more pronounced in Arctic tundra than boreal forest. This is due primarily to the comparatively large stature of the boreal forest canopy, which protrudes through the snow cover, reducing the effect of the presence or absence of snow (Betts & Ball 1997; Baldocchi *et al*. 2000). The degree to which snow cover affects the albedo of boreal ecosystems is a function of both the interception of snow (which differs between deciduous and evergreen species), and winter wind speeds. During the growing season, coniferous forest albedos are consistently low. Deciduous forests, however, have a relatively low albedo during early spring between snow melt and leaf-out, and again in autumn when the trees are bare but the surface is not yet snow-covered. In midsummer, deciduous forests have a higher albedo than the darker coniferous forests. Albedo tends to increase over the growing season (Ohmura 1981; 1982b; Blanken & Rouse 1994; Moore *et al*. 1994; Harding & Lloyd 1998), especially in sparsely vegetated ecosystems. The reason for this is that the albedo of bare soils, lichen and *Sphagnum* understoreys increases significantly when they dry out.

Largely due to predicted changes in albedo, it is estimated that the Earth's climate would be 2.6 °C warmer without snow and ice cover (Oerlemans & Bintanja 1995). The duration and location of snow cover and sea ice change K* at the surface, and are the dominant factors that govern the seasonal course of the radiation-budget (see (1)). In the northern hemisphere, the mean monthly land area covered by snow ranges from 7% to 40% during the annual cycle, making snow cover the most rapidly varying large-scale surface feature on Earth (Hall 1988).

Albedo differences among ecosystems. In addition to differences in winter albedo between tundra and boreal forest reported in the literature (e.g. Bonan *et al*. 1992; Foley *et al*. 1994), albedo differences between ecosystems in summer may be large enough to influence the surface energy balance, and ultimately climate. This would feed back to climate on the local, and possibly global, scale. The strongest summertime albedo differences exist between boreal forest with dark conifers (albedo around 0.09) and vegetated tundra (typically in the range 0.14–0.18, extremes within 0.10 and 0.22) (Table 4). Although this difference seems small, the net climate-forcing due to differences in absorbed global radiation between forest tundra and shrub tundra of northern Alaska are in the order of 5.5 W m^{-2} (Chapin *et al*. 1999), which is comparable to the effect of a doubling of global atmospheric CO_2 concentration (4.4 W m^{-2}, Wuebbles 1995). Fires and extensive logging activity have an even stronger impact on regional albedo differences as they dramatically decrease surface albedo.

3.3 Net radiation Q*

The net radiation at a surface, resulting from contributions by both the net short- and long-wave components (eqn 1) can be derived for large areas from satellite imagery with an accuracy between 8 and 41 W m^{-2} (Key *et al*. 1997b). The errors in estimating net radiation by remote sensing are primarily due to errors in the retrieval of surface temperature (which are accurate to within 0.3–2.1 K; Key *et al*. 1997a) and surface albedo. Net radiation estimates of similar or better accuracy can be obtained in small-scale ecosystem studies using a simple empirical model (Young & Woo 1997). Alternatively, since K↓ is more frequently measured than Q^*, it is useful to develop regression relationships between net and global radiation where the data are available, $Q^* = a + b$ K↓ (e.g. Davies 1967; Granger & Gray 1990; Saunders & Bailey 1994). The intercept a is a function of L^*. It differs strongly among sites (Table 4) due to regional differences in surface temperatures and cloudiness. Values range from −16 to −68 W m^{-2} in low Arctic tundra, and are generally less negative in the boreal forest, ranging from −3 to −29 W m^{-2}. The slope b is primarily a function of surface type: high values of 0.8–0.9 were found over dark surfaces like Toolik Lake or Jack pine forest, with typical values for tundra and nonconiferous boreal ecosystems between 0.6 and 0.7. Forest tundra falls between these two classes, and the slope for dry heath in Arctic tundra was lowest (Table 4).

The effect of clouds on Q^*, the cloud forcing, can be positive or negative, and arises through their contribution to L^*. A positive cloud forcing exists when the increase in greenhouse 'trapping' of long-wave radiation exceeds the reduction in short-wave radiation. High clouds with ice crystals have a net warming effect, while low clouds typically lead to a cooling. Satellite image analyses of the ERBE (Earth radiation budget experiment, e.g. Harrison *et al*. 1990) indicate that the boreal and Arctic regions north of 50° latitude show a negative radiative cloud forcing similar to the tropical region, i.e. clouds cool the surface, in contrast to the mid-latitudes, where clouds, on average, warm the surface. L^* is only slightly affected by clouds at high latitudes in contrast to the tropical zone. However, a substantial problem is that northern latitudes exhibit the largest errors in satellite-derived radiation fluxes, so that the precise role of cloud feedbacks in polar regions is uncertain (Curry *et al*. 1996).

4 Influences on energy partitioning and surface energy fluxes

An important question is, to what extent observed differences in energy partitioning and surface energy fluxes are due to differences in measurement conditions (e.g. specific weather conditions, time of season) rather than ecosystem properties. Differences in energy partitioning among ecosystem types in Table 4 are assumed to reflect both ecosystem properties and climate, whereas the spread of data within an ecosystem type is more likely due to interannual or intraseasonal variation in weather (cloudiness; advection of cold or warm air; see Rouse 2000) and correlated changes in soil moisture and temperature.

4.1 Influences of weather conditions

Differences between clear-sky conditions and cloudy or rainy weather permit an evaluation of ecosystem response to weather conditions. For example, water vapour pressure deficit is an important driving force for potential evapotranspiration (Penman 1948), and, during clear-sky conditions, it is always much higher than under cloudy conditions with low Q^*. However the sensitivity of fluxes to weather differs among ecosystem types. This is very evident when we compare alder steppe (Table 4, Ls5) with adjacent tussock tundra (Table 4, Lu10) in Alaska under sunny and cloudy conditions (Fig. 3). Measurements at these two sites were made simultaneously with similar instrumentation (Eugster *et al*. 1997) and similar topographic conditions, but the alder steppe had a greater abundance of shrubs.

Under cloudy conditions absolute values of Q_H and Q_E (Fig. 3) were similar between the two sites during the first half of the day, and differed only slightly during the second half. Under sunny conditions the absolute difference between sites was much greater. Alder steppe had significantly higher Q_H than tussock tundra throughout

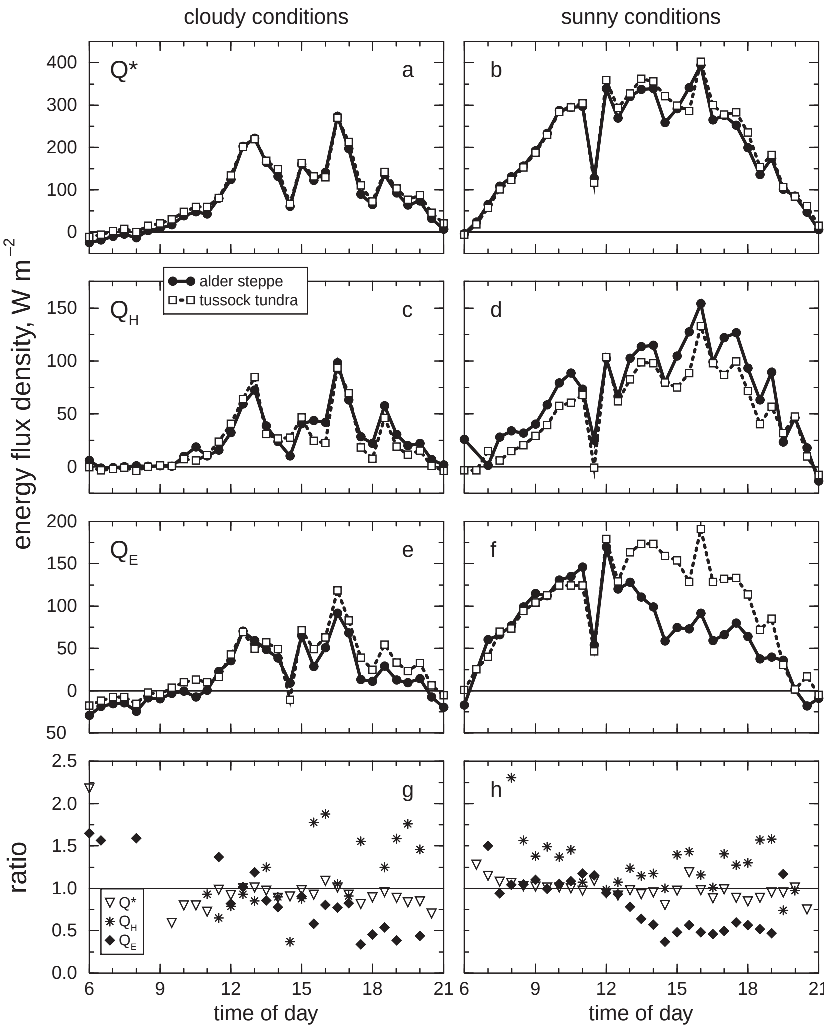

Fig. 3 Energy-partitioning differences between cloudy conditions (16 July 1996, left panels) and sunny conditions (17 July 1996, right panels) at an alder steppe site (Table 4, Ls5) and a tussock tundra site (Table 4, Lu10). Both sites are located within 750 m distance on a gentle slope in the foothills of the North Slope, Alaska. (a–f) Net radiation Q^*, sensible (Q_H) and latent (Q_E) heat flux densities; (g–h) Flux ratios of Q^*, Q_H and Q_E between the two sites for data pairs when absolute fluxes $> 10\,W\,m^{-2}$ at both sites. Local noon is at 14.00 hours.

the day (Fig. 3d), while Q_E remained similar between sites until two hours before local noon (Fig. 3f). After that, alder steppe showed a reduction in Q_E to 50% of the value of tussock tundra. Despite this great difference in flux densities, the ratio of fluxes between the two sites was almost independent of cloudiness (Fig. 3g–h).

4.2 Cold and warm air advection effects in coastal zones

The movement of a maritime air mass onto the adjacent land surface imports a mesoscale advective influence onto the terrestrial area. Whereas the Earth's surface is still responding primarily to local radiative effects and antecedent heating conditions, the advected air mass has its own characteristics. In northern coastal zones, these characteristics usually entail cold and moist air. This imposes steep temperature gradients between the terrestrial surface and overlying air and weak vapour pressure gradients. The result is an enhanced Q_H and diminished Q_E (Kozo 1982; Rouse 1984; 1991b; Weick & Rouse 1991a; Harazono *et al*. 1996; Rouse 2000).

Because ambient temperature has a strong influence on plant physiology, there is an important potential for feedbacks, especially during cold events where the vegetation temporarily becomes less active. This may reduce transpiration from plants and increase Q_H/Q^*. During warm events, the same vegetation type may show water stress that also results in stomatal closure, a reduction in transpiration and an increase in Q_H/Q^*. Thus at both temperature extremes we expect an increase in the fraction of available energy that is dissipated into Q_H rather than Q_E.

4.3 Seasonal trends and interannual variability

At present, there are insufficient data to identify any consistent regional differences in the seasonal trends of

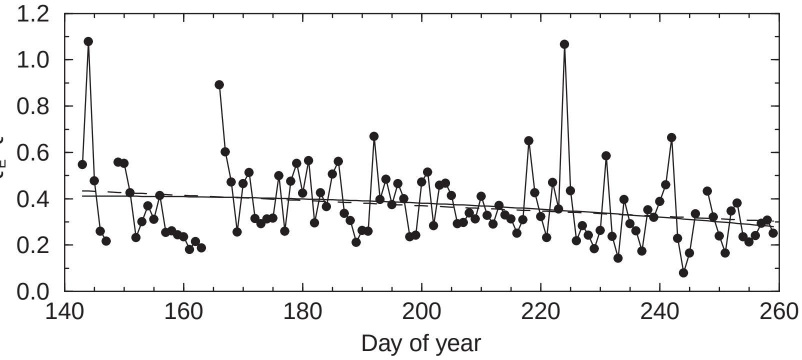

Fig. 4 Seasonal course of the ratio of the latent heat flux to net radiation (Q_E/Q^*, filled circles, $n = 113$) over an old Jack pine stand (data from Baldocchi *et al.* 1997). The full line is the quadratic fit $0.19 + (0.003 \times \text{DOY}) - (1.03 \times 10^{-5} \times \text{DOY}^2)$; the broken line indicates the linear trend $0.60 - (0.0011 \times \text{DOY})$.

the energy balance and energy partitioning in the Arctic and boreal zones. There was a clear drying out of the tundra in interior Canada (Blanken & Rouse 1994, 1995), and a less pronounced drying of boreal jack pine forest (Baldocchi *et al.* 1997; Fig. 4), shown by a decrease in Q_E/Q^* over the summer. In contrast, energy partitioning was rather constant on Svalbard (Harding & Lloyd 1998) during the snow-free period, and Ohmura (1984) reported a seasonal increase in Q_E/Q^*. Decreasing Q_E/Q^* (Blanken & Rouse 1994; Baldocchi *et al.* 1997; Fig. 4) are indicative of a strong control of surface and soil moisture over evapotranspiration, while Ohmura's (1984) results are best explained by atmospheric processes: warm air advection is more frequent in late season because surface temperatures are warmest in the second half of the growing season, which leads to warmer air temperatures than would be expected from concurrent net radiative input. This may explain why Q_H decreases over the season while Q_E increases in Ohmura's (1984) data.

The seasonal decrease of soil moisture appears to be an important factor in all cases considered here, leading to a seasonal decrease in Q_E/Q^*. This can be overridden by the opposite effect of warm air advection in sites close to the coast and depending on frequency of occurrence of such events.

4.4 Vegetation controls over transpiration

Energy partitioning at high latitudes is particularly sensitive to the proportion of the net energy that reaches the surface and is available for Q_G. The fraction Q_G/Q^* is heavily controlled by leaf area index (LAI) and stem area, which both influence the shading of the surface, and by surface albedo. Of the remaining energy, the second control is surface conductance G_s, or canopy resistance $R_c = 1/G_s$. The values for $G_{s,max}$ given in Table 4 were obtained by solving the Penman–Monteith equation (e.g. Jarvis & McNaughton 1986; Monteith & Unsworth 1990) for G_s during the approximately 6 h around mid-day when plant stomata are open. Priestley & Taylor (1972) used an empirical scaling factor to relate Q_E to equilibrium evaporation (Q_E; see Baldocchi *et al.* 2000). Stewart & Rouse (1977) found that the theoretical value $Q_E/Q_{E,eq} = 1.26$ is generally applicable to saturated surfaces in high latitudes. The data compiled in Table 4, however, show that $Q_E/Q_{E,eq}$ is clearly below this value in most Arctic and boreal ecosystems and that $Q_E/Q_{E,eq}$ decreases dramatically with increasing canopy resistance R_c (Fig. 5). The logistic fit (Fig. 5) to the data set yields a maximum value of $Q_E/Q_{E,eq}$ of 1.22 at low R_c, and a lower limit of 0.40 at high R_c. This confirms the high value supported by Stewart & Rouse (1977), but also reveals that Arctic and boreal ecosystems are generally much 'drier' than saturated surfaces without stomatal control of evaporation ($Q_E/Q_{E,eq} = 1.26$). Deciduous forest and bog show latent heat fluxes that correspond to equilibrium evaporation ($Q_E/Q_{E,eq} = 1$), while coniferous forests reduce transpiration by 50–75% of potential losses under calm conditions ($Q_E/Q_{E,eq}$ = 0.50–0.25 in Fig. 5). These energy savings are compensated by increased Q_H, which directly feeds back to air temperature and therefore also to the height of the atmospheric boundary layer (Baldocchi *et al.* 2000). Even the best numerical weather prediction models consistently overpredicted the transpiration rates over the boreal region before the BOREAS experiment (Sellers *et al.* 1997; Baldocchi *et al.* 2000) and thus led to an underestimation of local air temperatures, the depth of the atmospheric boundary layer, and turbulent convective mixing over boreal forest. A similar problem exists in tundra (Lynch, pers. comm.).

4.5 Energy partitioning of high-Arctic ecosystems

Energy fluxes of high-Arctic ecosystems cover a wide range (Fig. 6), from the wet and cool deep lakes with very small Q_H/Q^* to the dry low Arctic heath and the light taiga (pine and larch forests) where Q_H/Q^* is dominating the energy balance with values around 0.5. Figure 6 shows

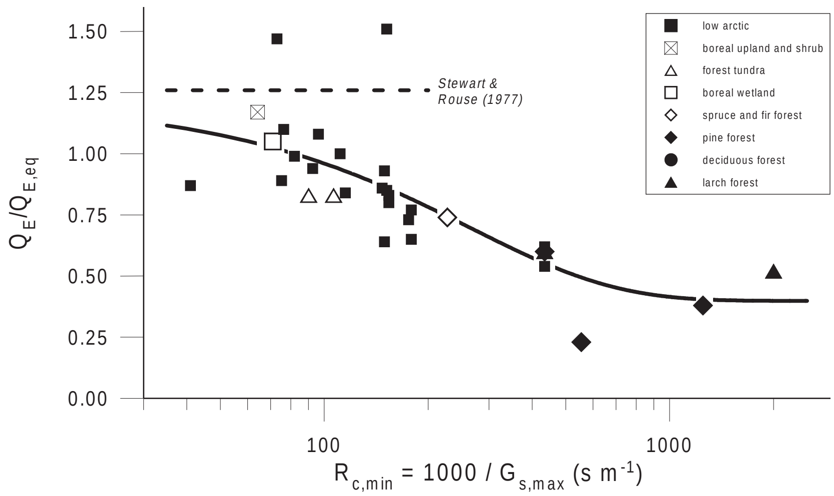

Fig. 5 Ratio between measured evapotranspiration (Q_E) and equilibrium evapotranspiration ($Q_{E,eq}$) as a function of minimum canopy resistance for selected Arctic and boreal ecosystems.

the statistical range of the relative energy fluxes for each vegetation class (Table 4), while Figs 7 and 8 display averaged diurnal cycles for selected representative sites in the boreal and tundra zones, respectively. The energy partitioning does not obey simple scaling laws (Fig. 6), although surface and soil moisture appears to be the most significant axis for describing the surface energy balance, followed by leaf area index (LAI, Fig. 6). Q_H/Q^* is strongly anticorrelated with the moisture gradient, while Q_G/Q^* is anticorrelated with LAI which shades the ground and thus reduces Q_G/Q^*. Q_E/Q^* reveals a complex pattern determined by both the moisture gradient, the LAI, and plant physiological controls over $R_{c,max}$ (Fig. 5). Thus, the highest values of Q_E/Q^* of high-latitude ecosystems are found in deciduous vegetation with low $R_{c,max}$ on sufficiently moist ground, while both wetter and drier conditions have less Q_E/Q^*.

Ellenberg (1996) uses moisture and soil pH as the two primary axes for explaining the optimum range of plant species and ecosystem types, an approach we were unable to follow due to the lack of information on soil pH for most sites. But it is known that soil pH is an important controller also in the Arctic (Walker *et al*. 1998). Additionally, the disturbance regime also plays an important role in managed ecosystems (Ellenberg 1996), which is also true for the boreal forest where the vegetation composition changes more rapidly due to logging activity than due to climatic change (Schulze, pers. comm.) or natural changes in fire frequency.

The ranges of energy partitioning are similar for Arctic and boreal ecosystems (Fig. 6) despite the differences in climate (Tables 1–3), therefore it is expected that the regional variation in energy partitioning and its feedback to climate are as important in the Arctic tundra as they are in the boreal forest, although this variation results from different ecosystem types in the two climate zones. For example, the energy partitioning of coastal wetlands in the Arctic is more similar to dark taiga (spruce and fir forest) than other wetlands, which do not differ between the two climate zones (Fig. 6). The available moisture of coastal wetlands is restricted by the shallow active layer over the permafrost, and Q_E/Q^* is further restricted by cold surface temperatures, while other Arctic and boreal wetlands behave more like freely evaporating surfaces (Fig. 5).

4.6 Comparison with other climate zones

The Bowen ratio,

$$\beta = Q_H/Q_E$$

is widely used for comparing the surface energy balance of climate zones and vegetation types with differing Q^*. The widest range of β was found for the light taiga and is comparable to the range found for grasslands in the FIFE study, which partially overlaps with the values found for semiarid areas (Table 5). The lowest β were found in deciduous boreal forests and noncoastal wetlands, and the values are comparable to the range of agricultural crops. Tropical oceans, tropical wet jungles with $\beta < 0.2$, and arid areas with $\beta > 3.8$ are the only ecosystem types that do not have a counterpart in the high-latitudes with similar energy partitioning characteristics (Table 5).

Again, as a special case, the energy partitioning of high and low Arctic coastal tundra differs considerably from real 'wetlands' (Table 5); it is comparable to a water-limited semiarid ecosystem, despite the high water table and the large fraction of open water that is present.

In temperate forest ecosystems the contribution of water loss from the forest floor is largely neglected because it contributes less than 10% to total Q_E in a temperate coniferous forest (Ellenberg 1996) and less than

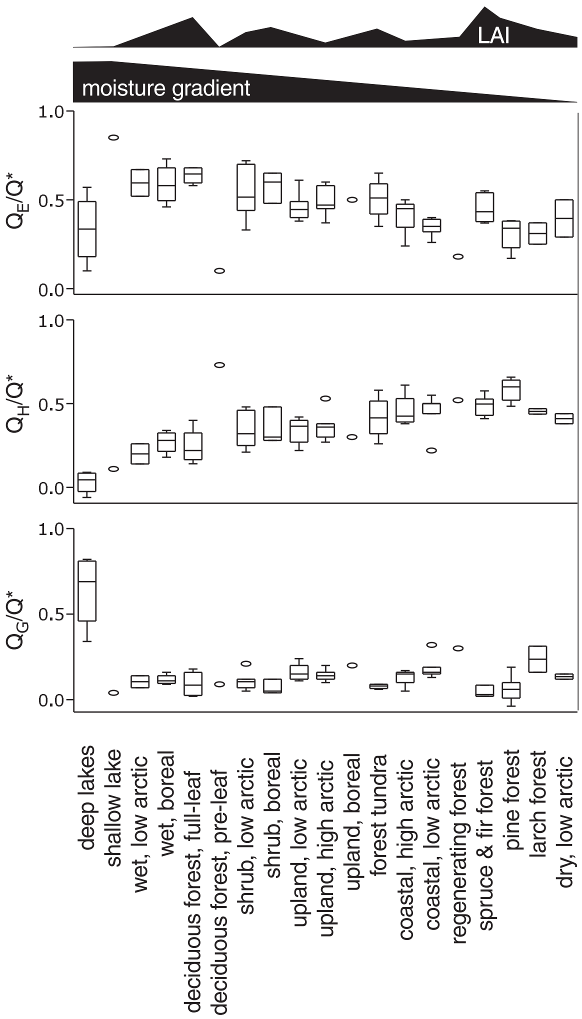

Fig. 6 Energy partitioning of northern ecosystems. Values are grouped according to the classification used in Table 4 and are sorted along the gradients of surface or soil moisture and leaf area index (LAI). The boxes of Q_E/Q^*, Q_H/Q^* and Q_G/Q^* show the interquartile range with the median value in the middle. Whiskers extend to the upper and lower adjacient values, and the outside values are plotted individually as ellipses.

5% of peak canopy evaporation fluxes in a temperate deciduous forest (Baldocchi & Vogel 1996). At high latitudes, however, the forest floor contribution is important (e.g. Lafleur 1992; Kelliher *et al*. 1997) and may be the dominant source of moisture flux (Baldocchi *et al*. 2000). Because wet moss surfaces can evaporate more water than open water surfaces (Firbas 1931), the dense moss or lichen covers typical of many boreal and Arctic ecosystems are an important controller of ecosystem water losses to the atmosphere (Rouse 2000; Arneth *et al*. 1996).

In summary, most ecosystems that occur across a broad climatic gradient (e.g. wet and shrub ecosystems) do not differ strikingly across this climatic gradient, suggesting that vegetation type exerts at least as strong an effect on energy partitioning as does climate.

5 Feedbacks to climate

Regional and local climate are strongly influenced by the energy partitioning at the surface, and local microclimatic conditions often differ considerably from the large-scale zonal climate. There is a complex system of interactions between local-scale energy exchange processes and larger-scale climate variables (Fig. 9). In this section the most important feedbacks between the surface energy balance and relevant components of the climate system are identified. Following this discussion, two examples of how landscape patchiness feeds back to microclimate are presented. The role of vegetation shifts and their potential feedbacks to climate are discussed at the end of this section, together with considerations about how the regional climate of high-latitudes may feed back to the global climate.

5.1 Interactions between albedo and soil moisture

Although it is well known that the presence of snow or ice has a great potential to feed back to local, regional and global climate (e.g. Gallimore & Kutzbach 1996) due to increased surface albedo (Curry *et al*. 1996), the effect of albedo is also significant during the snow-free season. Following snow-melt, increasing Q_E decreases the soil moisture content, which increases the surface albedo (Section 3.2; Fig. 9). Consequently, there is a decrease in Q^* at the surface as a result of reduced K*. In regions of exposed unvegetated soil or sparsely vegetated areas, water vapour losses via Q_E decrease under such conditions. The remaining net radiation is then partitioned into Q_H rather than Q_G, due to the poor thermal and hydraulic conductivity of the parched surface. This results in a feedback loop that preserves soil moisture at depth when the surface dries out. Conversely, in the case of substantially vegetated deciduous regions, the leaf-out process increases albedo, since the leaves are more reflective than the moist soil surface which they obscure. Although the impact on net radiation due to the increased albedo is similar to that of a drying unvegetated surface, the plant roots penetrate beyond the immediate dry surface, providing a link to subsurface moisture. Consequently, the rate at which moisture reserves are depleted, i.e. the relative partitioning of Q^* into Q_E is controlled more strongly by canopy conductance than by changes in albedo.

In summary, although there are discernable albedo related feedbacks to soil moisture availability in

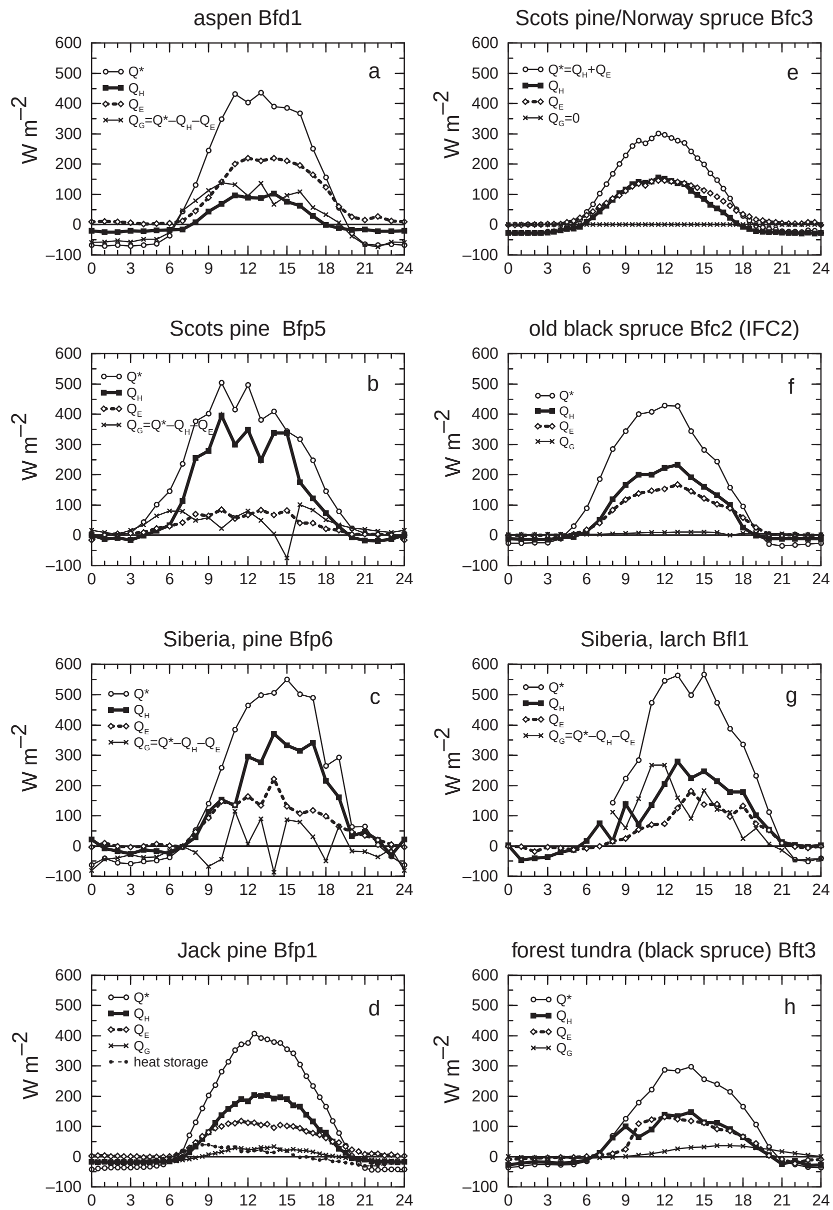

Fig. 7 Diurnal cycles of surface energy fluxes for selected boreal forest ecosystems: (a) deciduous forest; (b–f) evergreen coniferous forest; (g) deciduous coniferous forest; and (h) forest tundra. Site identifications correspond with Table 4.

unvegetated and vegetated ecosystems, neither ecosystem type is likely to suffer immediate desiccation.

5.2 Feedbacks to temperature and moisture

The role of permafrost. A change in the relative partitioning of Q^* into Q_H is the most direct pathway to change the temperature of the atmospheric boundary layer. Q_H is driven by the temperature gradient between the surface and the overlying air. Consequently, any process that increases this gradient will also warm the atmosphere. For example, Q_G increases the surface temperature, depending on the physical properties of the soil. However, if there is permafrost, a considerable amount of Q_G is used for melting permafrost during summer, which increases the depth of the active layer. This energy flux absorbed by the melt of ground ice is therefore not available for increasing surface temperatures. Hence a negative feedback from seasonal melt of permafrost to surface and soil temperature (Fig. 9), which also reduces the temperature gradient that drives Q_H.

This implies that the energy partitioning at the surface is buffered against changes in climatic forcing by changes in melting of permafrost. Therefore, the Arctic and Subarctic may not experience an immediate change in air temperature during the transition phase where permafrost disappears. However, by the time when permafrost has disappeared or is significantly deeper,

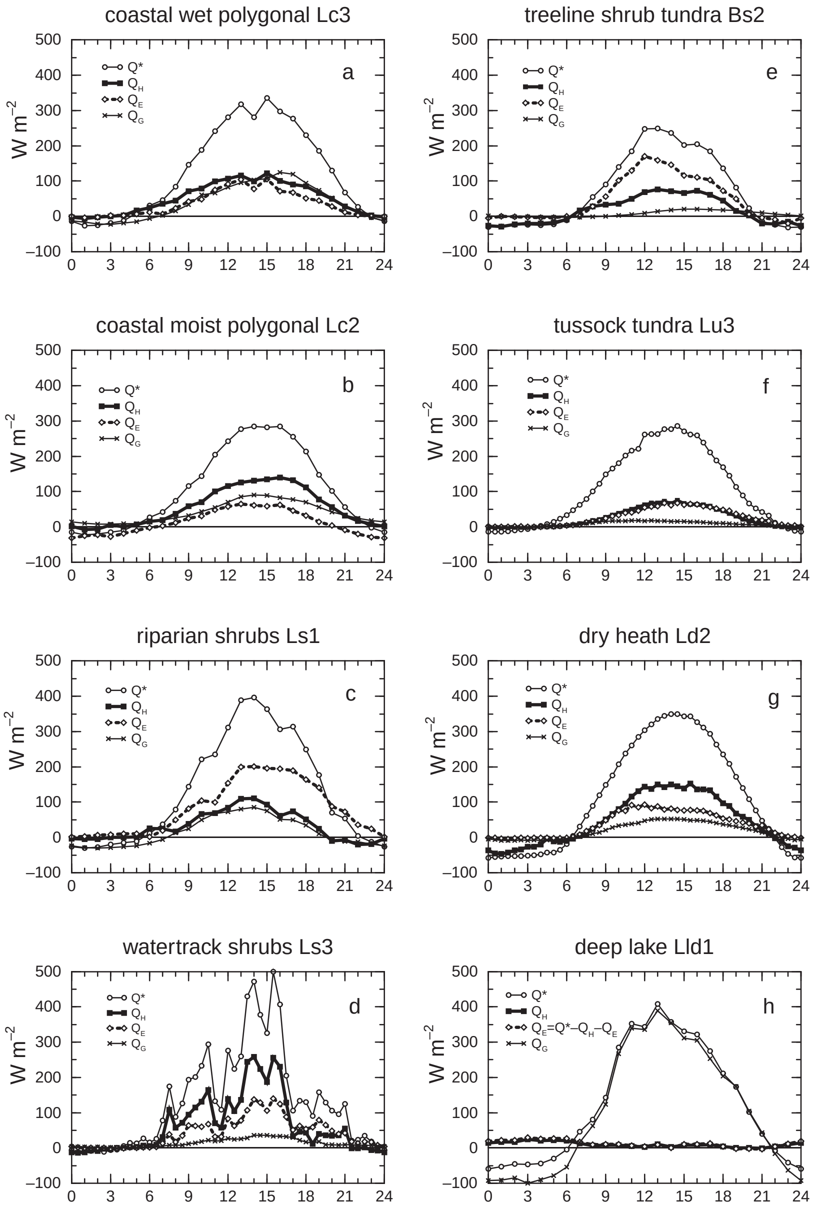

Fig. 8 Same as in Fig. 7 but for selected tundra ecosystems: (a–b) coastal tundra; (c–e) shrub tundra; (f) tussock tundra; (g) tundra heath; and (h) Arctic lake.

this important controlling mechanism would no longer be active. It is even possible that such a transition is nonreversible.

The deep planetary boundary layers over boreal forest. In the southern part of the boreal zone, there is no permafrost to buffer the influence that changes in surface energy partitioning impose on air temperatures. Therefore, as a result of reduced Q_E over coniferous forests in this region (Fig. 5), limited nutrient supply, leaf area and soil moisture (Baldocchi *et al.* 2000) the greatest proportion of Q^* is converted to Q_H. This increases air temperature (Fig. 9) and drives thermal convection that supports a deep planetary boundary layer. This deep convection exists over the whole boreal forest zone and might be important in controlling the summer position of the polar front (Pielke & Vidale 1995).

The role of clouds and water vapour. In substantially vegetated regions it is most likely that a change in the partitioning of available radiation into Q_H will be counteracted by a larger relative influence on Q_E than Q_G (Fig. 9). Therefore, it is possible that an ecosystem change that results in a reduction of Q_H would also cause an increase in atmospheric moisture content. Assuming that there is still sufficient mixing within the atmospheric boundary layer to bring the moister air to its lifting

Table 5 Ranges of Bowen ratios of Arctic and boreal ecosystem types in comparison with ranges typical of other climate zones

Ecosystem type	Range of Bowen ratios	Source
Tropical oceans	≈0.1	Oke (1987)
Tropical wet jungles	0.1–0.3	Oke (1987)
Agricultural crops	0.1–1.0	Valentini *et al*. (1999a)
Deciduous forests (full-leaf)	0.2–0.7	This study
Wetlands (Arctic and boreal)	0.2–0.7	This study
Temperate forests and grassland	0.4–0.8	Oke (1987)
Low Arctic shrub tundra	0.3–1.5	This study
Boreal shrub	0.5–1.0	This study
Low Arctic upland tundra	0.4–1.0	This study
Forest tundra	0.4–1.7	This study
Scots pine, southern Germany	0.6–1.4	Gay *et al*. (1996)
Dark taiga (spruce & fir)	0.7–1.5	This study
Low Arctic coastal tundra	0.6–2.1	This study
High Arctic coastal tundra	0.8–2.5	This study
Grassland FIFE	0.3–4.0	Valentini *et al*. (1999a)
Light taiga (pine & larch)	0.6–3.8	This study
Semiarid areas	2.0–6.0	Oke (1987)

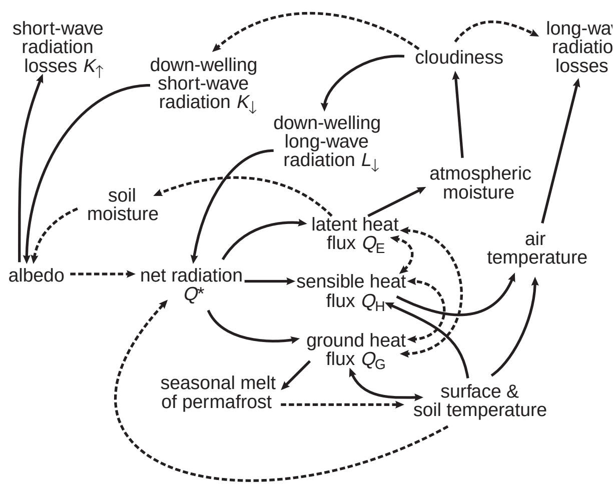

Fig. 9 Feedbacks between energy fluxes and relevant components of the climate system at high latitudes during the snow-free season. Positive feedbacks are indicated with full lines, negative feedbacks with broken lines.

condensation level, increased cloudiness would result. However, it is not known whether increased cloudiness also means higher or lower Q^* in the Arctic (Curry *et al*. 1996).

5.3 Feedbacks to microclimate in patchy terrain

Because of the complexity of the interactions between various components of the climate system (e.g. Fig. 9), and the additional complexity of landscape, it is necessary to use numerical models to integrate the nonlinear behaviour of this system and assess the importance of any of the feedback mechanisms that might exist. Two examples of results from numerical model simulations of the Arctic and the boreal zone show how local surface conditions can influence regional climate.

The patchiness of the land cover in tundra regions is due to topographically controlled variation in soil moisture availability and vegetation stature (Fig. 6) on spatial scales of < 100 m (Fig. 10a). As described in Section 2, such treeless tundra regions experience significant redistribution of snow by the wind, leading to spatially heterogeneous snow covers of varying depth and density. During snow melt, the variation in snow depth leads to a patchy mosaic of dark surfaces and bright snow patches that diminish as the snow melts (Fig. 10b–e). At the beginning of snow melt (Fig. 10b), snow accumulations are found in the valleys, and the thinnest snow layers exist along the wind-exposed western slopes. Snow melts first where it is most thinly distributed, on the vegetation-free surfaces (Fig. 10c), while deeper snow packs persist where shrubland or wet tundra vegetation had traped the snow (Liston 1995). The landscape pattern is determined by the combination of the instantaneous surface energy balance and the seasonal history of snow accumulation and redistribution during this period.

Variations in Q_H as a result of spatial variability in land surface type can produce mesoscale circulations if the surface heterogeneity occurs at horizontal scales between twice the convective boundary layer (CBL) height and twice the local Rossby radius (see Vidale *et al*. 1997). Differences in sensible heat fluxes of over 250 W m^{-2} were found on summer afternoons between

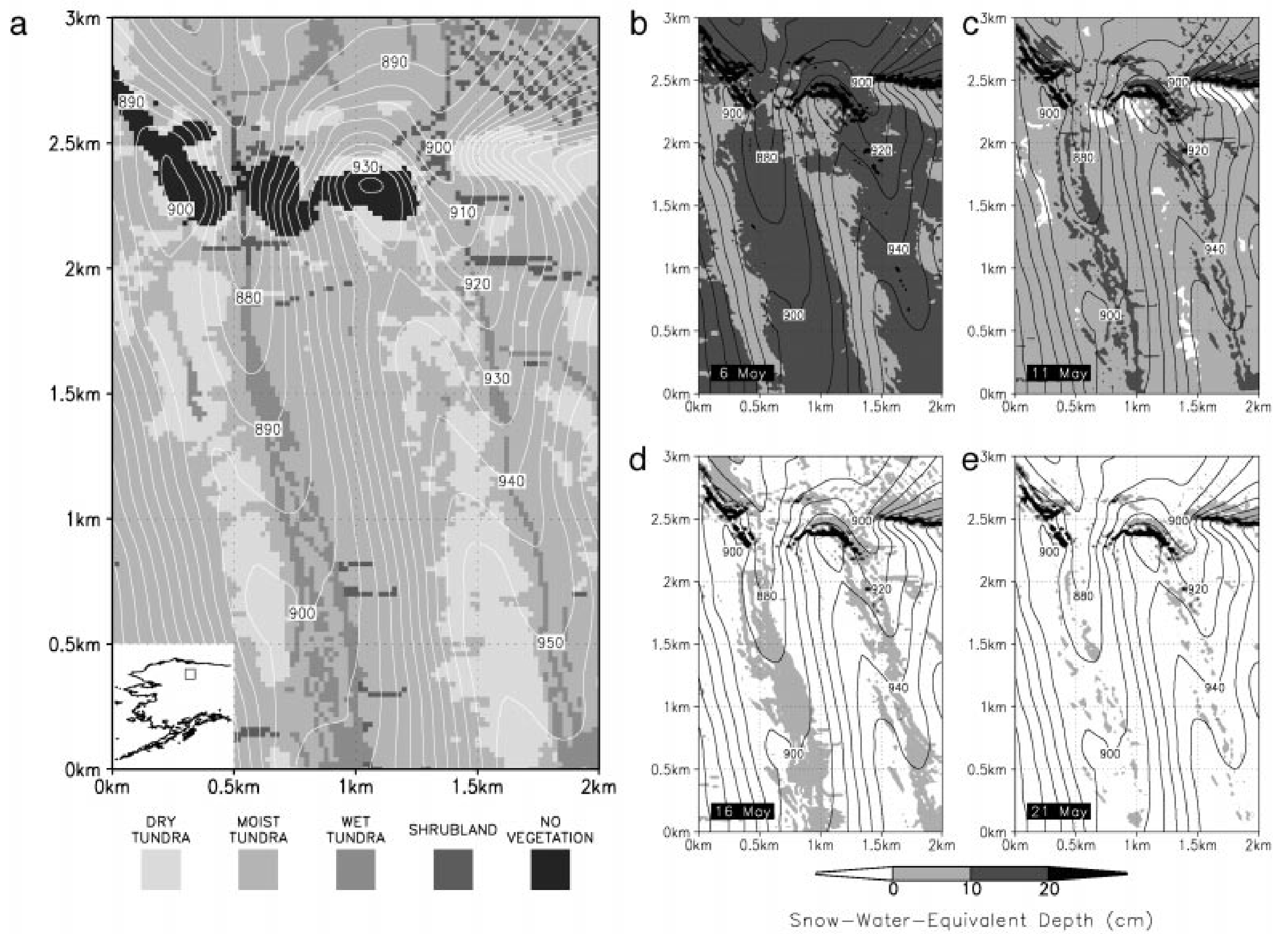

Fig. 10 Influence of the patchiness on snow melt: (a) vegetation and topography of Imnavait Creek, Arctic Alaska; (b) end-of-winter snow distribution for the Imnavait Creek Basin in arctic Alaska; (c–e) depletion of snow cover every five days during the snow-melt period (Liston & Sturm 1998). Solid lines are topographic contours (10 m interval). Prevailing wind direction in this region is from the south-west.

lakes and surrounding vegetation in both aircraft data (Sun *et al*. 1997) and model results (Vidale *et al*. 1997). The mesoscale flows generated in a patchy landscape are structurally similar to sea and land breezes (Vidale *et al*. 1997). Figure 11 shows a daytime lake breeze generated around Candle Lake in Canada under ≈10 m s^{-1} synoptic-scale winds. Significant mesoscale fluxes of heat, moisture and momentum are associated with these circulations, which can affect the overall atmospheric budgets even above the atmospheric boundary layer. Similarly, Taylor *et al*. (1998) found evidence of mesoscale flow between snow-covered lakes and surrounding forest in the boreal region of Canada.

The latitudinal extent of the boreal forest is strongly influenced by the fire regime at the southern limit (Hogg 1994). Schulze *et al*. (1999) and Valentini *et al*. (1999b) argue that the contrast between high evaporation from peat bogs in the neighbourhood of logging areas with low Q_E may lead to increased frequency of convective storms. These will increase fire frequency due to lightening, and thus disturb the southern limit of the boreal forest and its contribution to the continental water balance of Siberia.

5.4 Feedbacks between vegetation shifts and climate

Although numerical models are needed for assessing the importance of feedback processes in a complex system, it is often not known which level of detail such a model needs to represent. In order to identify the vegetation shifts that strongly change the energy balance of the surface, a set of vegetation change scenarios were generated based on reasonable assumptions of large-scale changes in climate forcing (Table 6) that were used to assess the relative potential for feedbacks in the surface energy budget (Fig. 12). For example, vegetation shift scenario 1, the conversion of high Arctic upland to low Arctic upland tundra (Table 6) does not change the

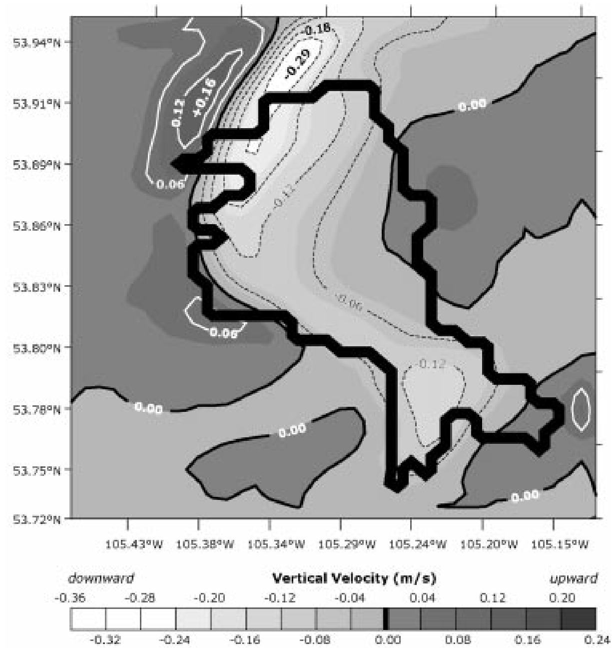

Fig. 11 Mesoscale circulation induced by a boreal lake. Horizontal cross-section of vertical velocity at 1250 m a.s.l. over Candle Lake, Canada (bold outline) for RAMS grid 3 at 19 UTC, 21 July 1994 (contour interval is $0.06\,\mathrm{m\,s^{-1}}$). Positive values are updrafts, negative values are downdrafts. A strong circulation cell exists, e.g. along the north-western lake shore with an updraft area over the land (dark shading) and an adjacent area (bright shading) with strong downdraft. Tick marks are in decimal degrees.

surface energy budget and is plotted in the centre of Fig. 12 where the unity lines cross. Deviations from this point indicate an amplification or a reduction of the imposed climate forcing by local feedback processes.

The most important changes in surface energy partitioning, and hence in the feedback to larger scales, is expected from a combined decrease in precipitation and in fire frequency (Fig. 12) which has the potential of converting deciduous forest to coniferous forest types (Table 6), and which would more than double Q_H by reducing Q_E to roughly 70% of today's value. If there is no decrease in precipitation, then both an increase and a decrease in fire frequency would damp the assumed temperature increase via a cooling feedback and make the atmosphere wetter by reducing Q_H and increasing Q_E. However, it has to be noted that if fire frequency increases, then an important transition period with a strong albedo feedback and thus warmer and drier conditions, may result before the new vegetation canopy is fully developed (see Section 3.2).

Although increased logging in forested areas is a factor that has a much more direct and measurable impact on the carbon budget of the boreal zone (Schulze *et al.* 1999) comparable to an increase in fire frequency, the energy balance feedbacks of logging appear to be very different from that of fires: the removal of the canopy increases the relative values of Q_G (Fig. 6) and decreases Q_E, while there is no siginificant effect on Q_H (Fig. 12). The reason for this is that Q_H/Q^* is already large in coniferous forests. Thus, the most important feedback to climate from logging can be expected in the atmospheric moisture budget and the hydrological balance, not in a direct feedback to air temperatures.

The spread of the data in Fig. 12 shows that there is little room for speculations of simultaneous reinforcements of both the temperature and the moisture feedback. It is much more likely that the feedback processes of vegetation shifts strongly influence the way how large-scale climate forcings are absorbed by these changes, or diverted from the temperatur axis to the moisture axis in Fig. 12, and *vice-versa*. It is essential to realize that an imposed temperature increase and change in precipitation, as is prediced by GCMs may become invisible due to counteracting changes in the surface energy budget, or they may be strongly amplified depending on the type of ecosystem. The vegetation shifts that revealed to be important controllers of these feedbacks are indicated in Table 6.

5.5 Implications for the energy redistribution on the globe

There is no doubt that the energy-balance feedbacks to climate discussed above are relevant on the local and regional scale. However, their significance for the global scale is not yet clearly understood. Already under current conditions there is a large energy flux from the warm equatorial zone toward the poles that drives the climate of the Earth. Overland *et al.* (1996) analysed 25 years of radiosonde data from the North Polar region north of 55°N and confirmed this generally known energy transport. Furthermore, their analyses showed that during summer large areas of the low Arctic and boreal zone are actually a heat source rather than a sink. For example, heat flows from Alaska in both northerly and easterly directions, and the energy flux from Siberia and Fennoscandia amplifies the general south-to-north flow and leads to stronger heat convergence in the eastern high Arctic north of Siberia than in the western high Arctic.

This redistribution of energy from certain regions in the Arctic and boreal zone to northern areas which is observed under current conditions may be increased under a warming climate whenever Q_H or Q_E increases. This is the case for most vegetation shift scenarios except the one with increased logging in forested areas (Fig. 12), which affects the hydrological cycle more significantly than the atmospheric energy transports.

Table 6 Energy-partitioning feedbacks of selected vegetation shifts for different climate forcing scenarios. Scenario assumptions: T+: increase in growing-season temperature and/or duration; *P*+(P-): increase (decrease) in growing-season precipitation; *F*+(F-): increase (decrease) in fire frequency; L+: increase in logging activity. Feedbacks: +T (−T): amplification (reduction) of the temperature feedback; +M (−M): amplification (reduction) of the moisture feedback; NS: not significant

ID	Current ecosystem	Replacement ecosystem	Climate forcing	Energy partitioning feedbacks to climate
1	High Arctic upland	Low Arctic upland	T+	NS
2	High Arctic coastal	Low Arctic coastal	T+	+T, −M, small
3	Low Arctic upland	Low Arctic shrub	T+(*P*+)	−T
4	Low Arctic upland	Low Arctic dry	T+(P−)	+T, −M, small
5	Low Arctic dry (heath)	Boreal upland	T+	−T, +M
6	Low Arctic shrub	Forest tundra	T+	+T
7	Low Arctic coastal	Low Arctic upland	T+, P−	−T, +M
8	Low Arctic coastal	Low Arctic wet	T+, *P*+	−T, +M, important
9	Low Arctic wet	Low Arctic upland	T+(P−)	+T, −M, important
10	Low Arctic wet	Boreal wet (bogs & mires)	T+, *P*+	+T
11	Boreal upland	Boreal shrub	*P*+	+M
12	Boreal shrub	Forest tundra	T+	+T, −M
13	Forest tundra	Spruce & fir forest	T+	+T, −M
14	Boreal wet (bog & mires)	Boreal shrub	T+(P−)	NS
15	Boreal wet (bog & mires)	Boreal shallow lake	*P*+	−T, +M, important
16	Spruce & fir forest	Deciduous forest	T+(*P*+), F−	−T, +M, important
17	Pine forest	Deciduous forest	T+(*P*+), F−	−T, +M, important
18	Spruce & fir forest	Boreal shrub	T+, *F*+	−T, +M, important
19	Pine forest	Boreal shrub	T+, *F*+	−T, +M, important
20	Deciduous forest	Spruce & fir forest	T+, P−, F−	+T, −M, important
21	Deciduous forest	Pine forest	T+, P−, F−	+T, −M, important
22	Deciduous forest	Boreal wet (bog & mires)	T+, *P*+, F−	+T, −M
23	Deciduous forest	Boreal shrub	T+, *F*+	+T
24	Larch forest	Boreal shrub	T+, *F*+	−T, +M, important
25	Spruce & fir forest	Regenerating forest	L+	−M, important
26	Pine forest	Regenerating forest	L+	−M, important
27	Larch forest	Regenerating forest	L+	−M, important

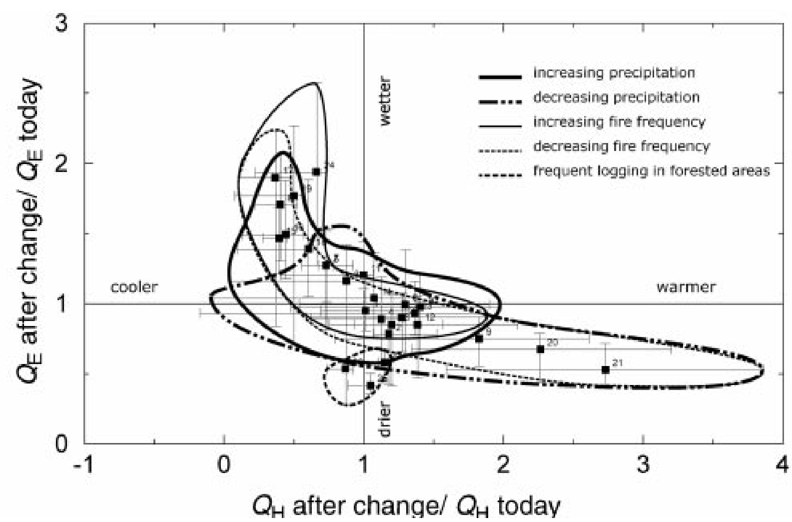

Fig. 12 Sensitivity of sensible (Q_H) and latent (Q_E) heat flux to the land-cover change scenarios in Table 6. The relative changes of the median values and the interquartile ranges are given for all cases in Table 6 (grey square and grey whiskers). The isolines encompass the cases with identical scenario assumptions.

6 Conclusions

Data on the surface energy balance from a variety of ecosystems representative of Arctic and boreal biomes were compiled from recent field experiments to describe the vegetation controls and influences on surface-energy partitioning. Interactions and feedbacks between the surface energy balance of ecosystems and summer climate were then discussed to assess the role that ecosystem properties and shifts in vegetation distribution may have on amplifying or damping climatic change in the Arctic and boreal regions, and what implications this might have for the global summer climate.

Great variation in relative fluxes of sensible heat, latent heat, and ground heat were observed, even between ecosystems that experience similar climate. The range of energy partitioning as a function of ecosystem type was found to be of similar order of magnitude in the Arctic and boreal zones.

Vegetation shift scenarios for the low Arctic and the boreal zone were found to play an important role for regional climate feedbacks, namely:

- low Arctic coastal tundra that is converted to wet tundra;
- low Arctic wet tundra if converted to upland (mesic) tundra;
- evergreen coniferous forest if converted to deciduous forest (and *vice-versa*);
- evergreen coniferous forest if converted to shrubland;
- the vegetation changes that result from logging the boreal forest.

The most important uncertainties for assessment of susceptibility and vulnerability of the boreal and Arctic ecosystems to climate change are (i) the uncertainty in cloud-feedback mechanisms (ii) the unknown magnitudes of changes in energy partitioning and whether vegetation shifts are likely to happen with the same time scale or not (iii) the complete lack of long-term energy-balance data from Siberia and the poor representation in the rest of the circumpolar boreal and Arctic zones, and (iv) the problems associated with the great variety of measuring and analyses techniques employed to obtain flux data.

Acknowledgements

This work resulted from a workshop on Arctic Boreal Processes That Feed Back to Climate, conducted at the National Center for Ecological Analysis and Synthesis, a Center funded by NSF (Grant #DEB-94–21535), the University of California at Santa Barbara, and the State of California. We'd like to thank Dr Dimitrios Gyalistras and Franziska Siegrist, University of Bern, for comments and suggestions on an early version of the manuscript, and the three anonymous reviewers for their substantial and constructive criticism. This final version was also strongly inspired and influenced by the discussions with the 1998 Dahlem Conference participants. Support for this paper was also provided to G. Liston and R. Pielke Sr. by NASA contracts NAG-5–7560 and NOAA contract NA67RJ0142.

References

Amiro BD, Wuschke EE (1987) Evapotranspiration from a boreal forest drainage basin using an energy balance/eddy correlation technique. *Boundary-Layer Meteorology*, **38,** 125–139.

Arneth A, Kelliher FM, Bauer G *et al*. (1996) Environmental regulation of xylem sap flow and total conductance of Larix gmelinii trees in eastern Siberia. *Tree Physiology*, **16** (1–2), 247–255.

Baldocchi DD, Kelliher FM, Black TA (2000) Climate and vegetation controls on boreal zone energy exchange. *Global Change Biology*, **6** (Suppl. 1), 69–83.

Baldocchi DD, Vogel CA (1996) Energy and CO_2 flux densities above and below a temperate broad-leaved forest and a boreal pine forest. *Tree Physiology*, **16,** 5–16.

Baldocchi DD, Vogel CA, Hall B (1997) Seasonal variation of energy and water vapor exchange rates above and below a boreal jack pine forest canopy. *Journal of Geophysical Research*, **102** (D24), 28,939–28,951.

Betts A, Ball JH (1997) Albedo over the boreal forest. *Journal of Geophysical Research*, **102** (D24), 28,901–28,909.

Black TA, den Hartog G, Neumann H *et al*. (1996) Annual cycles of CO_2 and water vapor fluxes above and within a Boreal aspen stand. *Global Change Biology*, **2,** 219–229.

Blanken PD, Black TA, Yang PC *et al*. (1997) Energy balance and canopy conductance of a boreal aspen forest: Partitioning overstory and understory components. *Journal of Geophysical Research*, **102,** 28,915–28,927.

Blanken PD, Rouse WR (1994) The role of willow-birch forest in the surface energy balance at arctic treeline. *Arctic and Alpine Research*, **26** (4), 403–411.

Blanken PD, Rouse WR (1995) Modelling evaporation from a high subarctic willow-birch forest. *International Journal of Climatology*, **15,** 97–106.

Bonan GB, Pollard D, Thompson SL (1992) Effects of boreal forest vegetation on global climate. *Nature*, **359,** 716–718.

Bonan GB, Davis KJ (1997) Comparison of the NCAR LSM1 land surface model with BOREAS aspen and jack pine tower fluxes. *Journal of Geophysical Research*, **102** (D24), 29,065–29,076.

Boudreau DL, Rouse WR (1995) The Role of Individual Terrain Units in the Water Balance of Wetland Tundra. *Climate Research*, **5,** 31–47.

Bowen IS (1926) The ratio of heat losses by conduction and by evaporation from any water surface. *Physical Review*, **27,** 779–787.

Chahuneau F, Desjardins RL, Brack E, Verdon R (1989) A micrometeorological facility for eddy flux measurements of CO_2 and H_2O. *Journal of Atmospheric and Oceanic Technology*, **6** (1), 193–200.

Chapin FS III, Eugster W, McFadden JP, Lynch AH, Walker DA (1999) Summer differences among arctic ecosystems in regional climate forcing. *Journal of Climate*, in press.

Curry JA, Rossow WB, Randall D, Schramm JL (1996) Overview of arctic cloud and radiation characteristics. *Journal of Climate*, **9** (8), 1731–1764.

Davies JA (1967) A Note on the Relationship Between Net Radiation and Solar Radiation. *Quarterly Journal of the Royal Meteorological Society*, **93,** 109–115.

Dethloff K, Rinke A, Lehmann R, Christensen JH, Botzet M, Machenhauer B (1996) Regional Climate Model of the Arctic Atmosphere. *Journal of Geophysical Research*, **101,** 23,401–23,422.

Edlund SA, Alt BT (1989) Regional congruence of vegetation and summer climate patterns in the Queen Elizabeth Islands, Northwest Territories, Canada. *Arctic*, **42,** 3–23.

Ellenberg H (1996). *Vegetation Mitteleuropas mit den Alpen in ökologischer, dynamischer und historischer Sicht*. 5th edn. Eugen Ulmer, Stuttgart, Germany.

Eugster W, McFadden JP, Chapin FS III (1997) A comparative approach to regional variation in surface fluxes using mobile eddy correlation towers. *Boundary-Layer Meteorology*, **85,** 293–307.

Fennessy MJ, Xue Y (1997) Impact of USGS Vegetation Map on GCM Simulations Over the United States. *Ecological Applications*, **7** (1)**,** 22–33.

Firbas F (1931) Untersuchungen über den Wasserhaushalt der Hochmoorpflanzen. *Jahrbuch für Wissenschaftliche Botanik*, **74,** 457–696.

Fitzjarrald DR, Moore KE (1992) Turbulent Transport Over Tundra. *Journal of Geophysical Research*, **97** (D15)**,** 16,717–16,729.

Fitzjarrald DR, Moore KE (1994) Growing season boundary layer climate and surface exchanges in a subarctic lichen woodland. *Journal of Geophysical Research*, **99** (D1)**,** 1899–1917.

Foley JA, Kutzbach JE, Coe MT, Levis S (1994) Feedbacks between climate and boreal forests during the Holocene epoch. *Nature*, **371,** 52–54.

Gallimore RG, Kutzbach JE (1996) Role of orbitally induced changes in tundra area in the onset of glaciation. *Nature*, **381,** 503–505.

Gay LW, Vogt R, Kessler A (1996) The May-October energy budget of a Scots Pine plantation at Hartheim, Germany. *Theoretical and Applied Climatology*, **53,** 79–94.

Goodison BE (1981) Compatibility of Canadian snowfall and snow cover data. *Water Resources Research*, **17,** 893–900.

Gorham E (1991) Northern peatlands: role in the carbon cycle and probable responses to climatic warming. *Ecological Applications*, **1,** 182–195.

Granger RJ, Gray DM (1990) A Net Radiation Model for Calculating Daily Snowmelt in Open Environments. *Nordic Hydrology*, **21,** 217–234.

Grelle A (1997) *Long-term water and carbon dioxide fluxes from a boreal forest: methods and applications.* Acta Universitatis Agricultureae Sueciae. PhD Thesis, University of Uppsala, Sweden.

Gyalistras D, Fischlin A (1999) Towards a general method to construct regional climatic scenarios for model-based impacts assessments. *Petermann's Geographische Mitteilungen*, **143,** 251–264.

Halldin S, Gottschalk L, van de Griend A *et al*. (1995). *Science Plan for NOPEX*. NOPEX Central Office, Institute of Earth Scienses, Uppsala University, Norbyvägen 18 B, SE-752 36 Uppsala, Sweden.

Hall DK (1988) Assessment of polar climate change using satellite technology. *Reviews of Geophysics*, **26** (1)**,** 26–39.

Harazono Y, Yoshimoto M, Miyata A, Uchida Y, Vourlitis GL, Oechel WC (1995) *Micrometeorological Data and their Characteristics over the Arctic Tundra at Barrow, Alaska during the Summer of 1993*. Miscellaneous publ. of the Nat. Inst. Agro-Environmental Sciences, Tsukuba, Japan, no. 16. (ISSN 0912–7542).

Harazono Y, Yoshimoto M, Vourlitis GL, Zulueta RC, Oechel WC (1996) Heat, Water and Greenhouse Gas Fluxes over the Arctic Tundra Ecosystems at Northslope in Alaska. *Proceedings IGBP/BAHC-LUCC joint inter-core projects symposium*, 4–7 November 1996, Kyoto, Japan, pp. 170–173.

Harding RJ, Lloyd CR (1998) Fluxes of water and energy from high latitude tundra sites in Svalbard. *Nordic Hydrology*, **29,** 267–284.

Harding RJ, Pomeroy JW (1996) The energy balance of the winter boreal landscape. *Journal of Climate*, **9,** 2778–2787.

Hare FK, Hay JE (1974) The climate of Canada and Alaska. In: *World Survey of Climatology* (eds Bryson RA, Hare FK), vol. 2, pp. 49–129. Elsevier, Amsterdam.

Hare FK, Thomas MK (1979). *Climate Canada*, 2nd edn. John Wiley and Sons, Toronto.

Harrison EF, Minnis P, Barkstrom BR, Ramanathan V, Cess RD, Gibson GG (1990) Seasonal variation of cloud radiative forcing derived from the Earth Radiation Budget Experiment. *Journal of Geophysical Research*, **95,** 18,687–18,703.

den Hartog G, Neumann HH, King KM, Chipanshi AC (1994) Energy budget measurements using eddy correlation and Bowen ratio techniques at the Kinosheo Lake tower site during the Northern Wetlands Study. *Journal of Geophysical Research*, **99,** 1539–1549.

Hogg (1994) Climate and the southern limit of the western Canadian boreal forest. *Canadian Journal of Forest Research*, **24,** 1835–1845.

Hollinger DY, Kelliher FM, Schulze ED *et al*. (1998) Forest-atmosphere carbon dioxide exchange in eastern Siberia. *Agricultural and Forest Meteorology*, **90,** 291–306.

Hurtalová T (1997) Self-preservation in the daily course of the surface energy balance. *Contributions of the Geophysical Institute of the Slovak Academy of Sciences. Series of Meteorology, Bratislava, Czechoslovakia*, **17,** 35–43.

Jacobs JD, Headley AN, Maus LA, Mode WN, Simms ÉL (1997) Climate and vegetation of interior lowlands of southern Baffin Island: long-term stability at the low Arctic limit. *Arctic*, **50** (2)**,** 167–177.

Jarvis PG, McNaughton KG (1986) Stomatal control of transpiration: scaling up from leaf to region. *Advances in Ecological Research*, **15,** 1–49.

Jarvis PG, Masseder JM, Hale SE, Moncrieff JB, Rayment M, Scott SL (1997) Seasonal Variation of carbon dioxide, water vapor and energy exchanges of a boreal black spruce forest. *Journal of Geophysical Research*, **102,** 28,953–28,966.

Keeling CD, Chin JFS, Whorf TP (1996) Increased activity of northern vegetation inferred from atmospheric CO_2 measurements. *Nature*, **382** (6587)**,** 146–149.

Kelliher FM, Hollinger DY, Schulze ED *et al*. (1997) Evaporation from an eastern Siberian larch forest. *Agricultural and Forest Meteorology*, **85** (3–4)**,** 135–147.

Kelliher FM, Lloyd J, Arneth A *et al*. (1998) Evaporation from a central Siberian pine forest. *Journal of Hydrology*, **205,** 279–296.

Key JR, Collins JB, Fowler C, Stone RS (1997a) High-latitude surface temperature estimates from thermal satellite data. *Remote Sensing of Environment*, **61** (2)**,** 302–309.

Key JR, Schweiger AJ, Stone RS (1997b) Expected uncertainty in satellite-derived estimates of the surface radiation budget at high latitudes. *Journal of Geophysical Research*, **102** (C7)**,** 15,837–15,847.

Keyser AR, Kimball JS, Nemani RR, Running SW (1999) Simulating the effects of climate change on the carbon balance of North American high latitude forests. *Global Change Biology*, **6** (Suppl. 1), 185–195.

Kittel TGF, Steffen WL, Chapin FS III (1999) Global and regional modeling of arctic-boreal vegetation distribution and its sensitivity to altered forcing. *Global Change Biology*, **6** (Suppl. 1), 1–18.

Kobak KI, Turchinovich IY, Kondrsheva Yu N, Schulze ED, Schulze W, Koch H, Vygodskaya NN (1996) Vulnerability and adaptation of the larch forest in Eastern Siberia in climate change. *Water Air and Soil Pollution*, **92** (1–2), 119–127.

Kozo TL (1982) An observational study of sea breezes along the Alaskan Beaufort Sea Coast: Part I. *Journal of Applied Meteorology*, **21** (7), 891–905.

Lafleur PM (1992) Energy balance and evapotranspiration from a subarctic forest. *Agricultural and Forest Meteorology*, **58**, 163–175.

Lafleur PM, Rouse WR (1995) Energy partitioning at treeline forest and tundra sites and its sensitivity to climatic change. *Atmosphere-Ocean*, **33**, 121–133.

Lafleur PM, Rouse WR, Carlson DW (1992) Energy balance differences and hydrologic impacts across the northern treeline. *International Journal of Climatology*, **12**, 193–203.

Liston GE (1995) Local advection of momentum, heat, and moisture during the melt of patchy snow covers. *Journal of Applied Meteorology*, **34** (7), 1705–1715.

Liston GE, Sturm M (1998) A snow-transport model for complex terrain. *Journal of Glaciology*, **44** (148), 498–516.

Lynch A, Chapman W, Walsh J, Weller G (1995) Development of a Regional Climate Model of the Western Arctic. *Journal of Climate*, **8**, 1556–1570.

Marsh P (1991) Water flux in melting snow covers. In: *Advances in Porous Media* (ed. Corapcioglu MY), Vol. 1, pp. 61–124. Elsevier, Amsterdam.

McFadden JP, Chapin FS, IIIHollinger DY (1998) Subgrid-scale variability in the surface energy balance of arctic tundra. *Journal of Geophysical Research*, **103** (D22), 28,947–28,961.

Monteith JL, Unsworth MH (1990) *Principles of Environmental Physics*, 2nd edn. Edward Arnold, London.

Moore KE, Fitzjarrald DR, Wofsy SC, Daube BC, Munger JW, Bakwin PS, Crill P (1994) A season of heat, water vapor, total hydrocarbon, and ozone fluxes at a subarctic fen. *Journal of Geophysical Research*, **99**, 1937–1952.

Nelson FE, Shiklomanov NI, Mueller GR, Hinkel KM, Walker DA, Bockheim JG (1997) Estimating active-layer thickness over a large region: Kuparuk River basin, Alaska, U.S.A. *Arctic and Alpine Research*, **29** (4), 367–378.

Oechel W, Hastings SJ, Vourlitis G, Jenkins M, Riechers G, Grulke N (1993) Recent change of Arctic tundra ecosystems from a net carbon dioxide sink to a source. *Nature*, **361**, 520–523.

Oerlemans J, Bintanja R (1995) *Snow and Ice Cover and Climate Sensitivity. The Role of Water and the Hydrological Cycle in Global Change.* NATO ASI Series, Vol. 131, pp. 189–198. Springer, Berlin.

Ohmura A (1981) *Climate and Energy Balance of Arctic Tundra*. Zürcher Geographische Schriften/ETH Zürich, Switzerland.

Ohmura A (1982a) A Historical Review of Studies on the Energy Balance of Arctic Tundra. *Journal of Climatology*, **2**, 185–195.

Ohmura A (1982b) Climate and Energy Balance on the Arctic Tundra. *Journal of Climatology*, **2**, 65–84.

Ohmura A (1982c) Evaporation from the surface of the arctic tundra on Axel Heiberg Island. *Water Resources Research*, **18** (2), 291–300.

Ohmura A (1982d) Regional water balance on the arctic tundra in summer. *Water Resources Research*, **18** (2), 301–305.

Ohmura A (1984) Comparative Energy Balance Study for Arctic Tundra, Sea Surface, Glaciers and Boreal Forests. *Geojournal*, **8** (3), 221–228.

Ohmura A, Gilgen H (1993a) Global energy balance archive (GEBA, WCP-water A7) and new aspects of the global radiation distribution on the Earth's surface. In: *IRS '92: Current Problems in Atmospheric Radiation* (eds Keevallik S, Kärner O), Hampton, VA, A. Deepak Publishing, 271–274.

Ohmura A, Gilgen H (1993b) Re-evaluation of the global energy balance. *Geophysical Monograph*, **75**, 93–110.

Ohmura A, Gilgen H, Wild M (1989) Global energy balance archive (GEBA). Zürcher Geographische Schriften, **34**, 1–62.

Oke TR (1987) *Boundary Layer Climates*. 2nd edn. Methuen, London.

Overland JE, Turet P, Oort AH (1996) Regional variation of moist static energy flux into the Arctic. *Journal of Climate*, **9**, 54–65.

Pattey E, Desjardins RL, St-Amour G (1997) Mass and energy exchanges over a black spruce forest during key periods of BOREAS 1994. *Journal of Geophysical Research*, **102**, 28,967–28,975.

Penman HL (1948) Natural evaporation from open water, bare soil and grass. *Proceedings of the Royal Society of London A*, **193**, 120–145.

Pielke RA, Cotton WR, Walko RL *et al*. (1992) A Comprehensive Meteorological Modeling System – RAMS. *Meteorology and Atmospheric Physics*, **49**, 69–91.

Pielke RA, Vidale PL (1995) The boreal forest and the polar front. *Journal of Geophysical Research*, **100**, 25,755–25,758.

Pitman AJ (1995) Simulating heterogeneous vegetation in climate models. Identifying when secondary vegetation becomes important. In: *Scale Issues in Hydrological Modelling* (eds Kalma JD, Sivapalan M), pp. 475–484. Advanstar Communications, Chichester.

Pomeroy JW, Gray DM (1994) Sensitivity of snow relocation and sublimation to climate and surface vegetation. In: *Snow and Ice Covers; Interactions with the Atmosphere and Ecosystems* (eds Jones HG *et al*.), IAHS Publication no. 223, pp. 213–226. IAHS, Wallingford.

Priestley CHB, Taylor RJ (1972) On the assessment of surface heat flux and evaporation using large-scale parameters. *Monthly Weather Review*, **100**, 81–92.

Raupach MR, Baldocchi DD, Bolle H-J *et al*. (1999) How is the atmospheric coupling of land surfaces affected by topography, complexity in landscape patterning, and the vegetation mosaic? In: *Integrating Hydrology, Ecosystems Dynamics, and Biogeochemistry in Complex Landscapes* (eds Tenhunen JD, Kabat P), Dahlem Workshop Report, pp. 177–196. John Wiley, Chichester.

Rinke A, Dethloff K, Christensen JH, Botzet M, Machenhauer B (1997) Simulation and validation of Arctic radiation and clouds in a regional climate model. *Journal of Geophysical Research*, **102** (D25), 29,833–29,847.

Rott H, Obleitner F (1992) The Energy Balance of Dry Tundra In West Greenland. *Arctic and Alpine Research*, **24**, 352–362.

Rouse WR (1984) Microclimate at Arctic tree line, Part 3, Effects of regional advection on the surface energy balance of upland tundra. *Water Resources Research*, **20** (1), 74–78.

Rouse WR (1993) Northern climates. In: *Canada's Cold Environments* (eds French H, Slaymaker O), pp. 65–92. McGill-Queens Press, Montreal.

Rouse WR (1998) A water balance model for a subarctic sedge fen and its application to climatic change. *Climatic Change*, **38,** 207–234.

Rouse WR (2000) The energy and water balance of high latitude wetlands: controls and extrapolation. *Global Change Biology*, **6** (Suppl. 1), 59–68.

Rouse WR, Carlson DW, Weick EJ (1992) Impacts of summer warming on the energy and water balance of wet tundra. *Climatic Change*, **22,** 305–326.

Rouse WR, Douglas MSV, Hecky RE *et al*. (1997) Effects of climate change on fresh waters of Arctic and subarctic North America. *Hydrologic Processes*, **11,** 873–902.

Saunders IR, Bailey WG (1994) Radiation and Energy Budgets of Alpine Tundra Environments of North America. *Progress in Physical Geography*, **18** (4)**,** 517–538.

Scherer D (1992) Klimaökologie und Fernerkundung: Erste Ergebnisse der Messkampagnen 1990/1991. *Stuttgarter Geographische Studien*, **117,** 89–104.

Scherer D, Parlow E, Ritter N, Siegrist F (1993) Klimaökologie und Fernerkundung. In: *Methoden- und Datenübersicht der Forschungsgruppen der Geowissenschaftlichen Spitzbergen-Expeditionen 1990 und 1991 zum Liefdefjorden (Datenband)* (ed. Leser H). Materialien zur Physiogeographie, 15, 51–58; appendix 121–151.

Schulze ED, Lloyd J, Kelliher FM *et al*. (1999) Productivity of forests in the Eurosiberian boreal region and their potential to act as a carbon sink – a synthesis. *Global Change Biology*, **5** (6), 703–722.

Schulze ED, Schulze W, Kelliher FM *et al*. (1995) Aboveground biomass and nitrogen nutrition in a chronosequence of pristine Dahurian Larix stands in eastern Siberia. *Canadian Journal of Forest Research*, **25** (6)**,** 943–960.

Sellers PJ, Hall FG, Kelly RD *et al*. (1997) BOREAS in 1997: Experiment overview, scientific results, and future directions. *Journal of Geophysical Research*, **102** (D24)**,** 28,731–28,769.

Stewart RB, Rouse WR (1977) Substantiation of the Priestly and Taylor parameter $\alpha = 1.26$ for potential evaporation in high latitudes. *Journal of Applied Meteorology*, **16** (6), 649–650.

Sun J, Lenschow DH, Mahrt L *et al*. (1997) Lake-induced atmospheric circulations during BOREAS. *Journal of Geophysical Research*, **102** (D24)**,** 29,155–29,166.

Tao X, Walsh JE, Chapman WL (1996) An assessment of global climate model simulations of Arctic air temperatures. *Journal of Climate*, **9** (5)**,** 1060–1076.

Taylor CM, Harding RJ, Pielke RA Sr *et al*. (1998) Snow breezes in the boreal forest. *Journal of Geophysical Research*, **103** (D18), 23,087–23,101.

Tchebakova NM, Parfenova EI, Vikhov VV (1992) Ecological parameters of the upper treeline in the Sayan Mountain range. In: *Proc Xth All-Union Conference On Upland Flora and Vegetation Research, Central Botanical Garden SB RAS, Novosibirsk*, pp. 103–104 (in Russian). Central Botanical Garden SBRAS, Novobirsk.

Thannheiser D (1992) Vegetationskartierungen auf der Germaniahalvøya. *Stuttgarter Geographische Studien*, **117,** 141–160.

Valentini R, Baldocchi DD, Tenhunen JD (1999a) Ecological Controls on Land–surface Atmospheric Interactions. In: *Integrating Hydrology, Ecosystems Dynamics, and Biogeochemistry in Complex Landscapes* (eds Tenhunen JD, Kabat P), Dahlem Workshop Report, pp. 117–145. John Wiley, Chichester.

Valentini R, Dore S, Marchi G *et al*. (1999b) Carbon and water exchanges of two contrasting Central Siberian landscape types: regenerating forest and bog. *Functional Ecology*, in press.

Vidale PL, Pielke RA, Steyaert LT, Barr A (1997) Case study modeling of turbulent and mesoscale fluxes over the BOREAS region. *Journal of Geophysical Research*, **102** (D24)**,** 29,167–29,188.

Vourlitis GL, Oechel WC (1999) Eddy covariance measurements of net CO_2 flux and energy balance of an Alaskan moist-tussock tundra ecosystem. *Ecology*, **80** (2), 686–701.

Vourlitis GL, Oechel WC (1997) Landscape-scale CO_2, H_2O Vapour and Energy Flux of Moist-wet Coastal Tundra Ecosystems over two Growing Seasons. *Journal of Ecology*, **85,** 575–590.

Vygodskaya NN, Milyukova I, Varlagin A *et al*. (1997) Leaf conductance and CO_2 assimilation of Larix gmelinii growing in an eastern Siberian boreal forest. *Tree Physiology*, **17** (10)**,** 607–615.

Walker DA (2000) Arctic tundra: interactions with climate, geology and topography. *Global Change Biology*, **6** (Suppl. 1), 19–34.

Walker DA, Auerbach NA, Bockheim JG *et al*. (1998) Energy and trace-gas fluxes across a soil pH boundary in the Arctic. *Nature*, **394,** 469–472.

Walsh JE, Lynch A, Chapman W, Musgrave D (1993) A Regional Model for the Atmosphere-Ice–Ocean Interaction in the Western Arctic. *Meteorology and Atmospheric Physics*, **51,** 179–194.

Weick EJ, Rouse WR (1991a) Advection in the coastal Hudson Bay lowlands, Canada. I: The terrestrial surface energy balance. *Arctic and Alpine Research*, **23** (3)**,** 328–337.

Weick EJ, Rouse WR (1991b) Advection in the coastal Hudson Bay lowlands, Canada. II: Impact of atmospheric divergence on the surface energy balance. *Arctic and Alpine Research*, **23** (3)**,** 338–348.

Weller G, Chapin FS III, Everett KR *et al*. (1995) The Arctic Flux Study: a regional view of trace gas release. *Journal of Biogeography*, **22,** 365–374.

Wild M, Ohmura A, Gilgen H, Roeckner E (1995) Validation of general circulation model radiative fluxes using surface observations. *Journal of Climate*, **8** (5)**,** 1309–1324.

Wild M, Ohmura A, Cubasch U (1997) GCM-simulated surface energy fluxes in climate change experiments. *Journal of Climate*, **10** (12), 3093–3110.

Woo MK, Lewkowicz AG, Rouse WR (1992) Response of the Canadian permafrost environment to climatic change. *Physical Geography*, **134,** 287–317.

Woo MK, Heron R, Marsh P, Steer P (1983) Comparison of weather station snowfall with winter snow accumulation in high arctic basins. *Atmosphere-Ocean*, **21,** 312–325.

Wuebbles DJ (1995) Air Pollution and Climate Change. In: *Composition, Chemistry, and Climate of the Atmosphere* (ed. Singh HB), pp. 480–518. Van Nostrand Reinhold, New York.

Yoshimoto M, Harazono Y, Miyata A, Oechel WC (1996) Micrometeorology and Heat Budget over the Arctic Tundra at Barrow, Alaska in the Summer of 1993. *Journal of Agricultural Meteorology*, **52,** 11–20.

Young SB (1971) The vascular flora of St. Lawrence Island with special reference to floristic zonation in the Arctic regions. *Contributions from the Grey Herbarium*, **201,** 11–115.

Young KL, Woo M-K (1997) Modelling Net Radiation in a High Arctic Environment Using Summer Field Camp Data. *International Journal of Climatology*, **17,** 1211–1229.

Zimov SA, Voropaev YV, Semiletov IP *et al*. (1997) North Siberian lakes: a methane source fueled by Pleistocene carbon. *Science*, **277,** 800–802.